U.PORTO

FACULDADE DE CIÊNCIAS
UNIVERSIDADE DO PORTO

MSc

2.º
CICLO

FCUP
ICBAS
UAB-IBB
2017

U.PORTO

Pharmacological chaperones to prevent transthyretin amyloidosis

Francisca Garcia Carvalho Pinheiro

FC

U.PORTO

FACULDADE DE CIÊNCIAS
UNIVERSIDADE DO PORTO

U.PORTO

INSTITUTO DE CIÊNCIAS BIOMÉDICAS ABEL SALAZAR
UNIVERSIDADE DO PORTO

UAB
Universitat Autònoma
de Barcelona

ibb
Institut de Biotecnologia
i de Biomedicina

Pharmacological chaperones to prevent transthyretin amyloidosis

Francisca Pinheiro

Master's dissertation presented to Faculdade de Ciências da Universidade do Porto and Instituto de Ciências Biomédicas Abel Salazar

Biochemistry

2017

Pharmacological chaperones to prevent transthyretin amyloidosis

Francisca Pinheiro

Master in Biochemistry
Department of Chemistry and Biochemistry
2017

Supervisors
Prof. Salvador Ventura, team leader, Institut de Biomedicina i Biotecnologia, Universidad Autònoma de Barcelona, Barcelona

Dr. Irantzu Pallarès, tenure-track lecturer, Institut de Biomedicina i Biotecnologia, Universidad Autònoma de Barcelona, Barcelona

Cosupervisor
Prof. Rosário Almeida, associate professor, Instituto de Investigação e Inovação em Saúde, Universidade do Porto, Porto

Universitat Autònoma de Barcelona

ibb Institut de Biotecnologia i de Biomedicina

U.PORTO

INSTITUTO DE CIÊNCIAS BIOMÉDICAS ABEL SALAZAR
UNIVERSIDADE DO PORTO

U.PORTO

FACULDADE DE CIÊNCIAS
UNIVERSIDADE DO PORTO

Todas as correções determinadas pelo júri, e só essas, foram efetuadas.

O Presidente do Júri,

Porto, _____/_____/_____

I. Acknowledgments

First of all, I would like to express my gratitude to the people that, in one way or another, were part of this process.

To my supervisor, Prof. Salvador Ventura, thank you for giving me the opportunity to be part of this group, for pushing me to be better and for trusting on my capabilities.

To Dr. Irantzu Pallarès, for the teaching, guidance and patience, but most of all, for the friendship.

To Prof. María Rosario Fernández, thank you for the warm welcome when I first arrived at this laboratory. I will not forget your kindness.

To those who worked with me, thank you for your helpful tips and for making work much easier. A special thanks to Jaime for the precious help and companionship and to Jordi, Samuel, Valentin, Anita and Cristina for the moments we shared.

To my closest friends and flat mates, Julia and Jessica, for listening my worries and making me laugh. You gave me strength to handle with the most difficult days.

To my supervisor in Portugal, Prof. Rosário Almeida, for always being available and for the useful tips.

To my Portuguese friends, for never stopping believing on me. To Joana, João and Rúben, for caring and understanding. To Bárbara and Leandro, for all the conversations, support and fun times.

Last, but not least, to my parents and sister, without whom I would not exist. Thank you for giving me the wings to fly and the anchor when falling. Thank you for always being by my side and for always making me see the bright side of things. You are my everything.

II. Abstract

Transthyretin is one of the proteins responsible for the transport and delivery of thyroxine and retinol to cells, in humans. It is an homotetramer mainly produced in the liver and in brain's choroid plexus, being secreted in the plasma and cerebrospinal fluid, respectively. Transthyretin aggregation is linked to senile systemic amyloidosis, familial amyloid cardiomyopathy, familial amyloid polyneuropathy and familial leptomeningeal amyloidosis. Currently, the main therapy for these amyloidosis is liver or combined liver and heart transplantation. However, there are many problems associated with this strategy, among them the fact that it is not an option for leptomeningeal amyloidosis. One approach that has been gaining power is based on the kinetic stabilization of the native protein, as tetramer dissociation is the rate-limiting step on transthyretin aggregation. In a recent work, we have repurposed tolcapone, a molecule approved by the United States Food and Drug Administration for Parkinson's Disease, as a potent transthyretin aggregation inhibitor. Noteworthy, tolcapone is able to cross the blood-brain barrier and it can become the first pharmacological treatment available for familial leptomeningeal amyloidosis, a rare type of transthyretin amyloidosis that affects the Central Nervous System. To explore this hypothesis, we used four transthyretin variants associated with familial leptomeningeal amyloidosis, A25T, L12P, V30G and Y114C. We characterized them in detail and were able to evaluate the activity of tolcapone for all of them. We observed that these variants are extremely unstable and that they affect the quaternary structure of the protein to different extents. Nevertheless, we demonstrated that tolcapone binds with high affinity to all the variants and establishes similar interactions to the ones reported for the WT protein. Importantly, we obtained evidences that tolcapone can stabilize their structure, preventing aggregation, as long as the quaternary structure is not completely lost. The results of this study emphasize the enormous potential of tolcapone, which seems to be the only option for patients with familial leptomeningeal amyloidosis, at least nowadays. Furthermore, the aspects that differentiate tolcapone from the other inhibitors, making it such a powerful drug for the transthyretin amyloidosis, prompt the use of tolcapone as a scaffold for redesigning even more effective derivates.

Key-words: protein aggregation, transthyretin amyloidosis, familial leptomeningeal amyloidosis, drug repositioning, tolcapone, kinetic stabilization, therapeutic strategy.

III. Resumo

A transtirretina é uma das proteínas responsáveis pelo transporte e entrega de tiroxina e retinol às células, em humanos. É um homotetramero produzido maioritariamente no fígado e no plexo coróide do cérebro, sendo secretado no plasma e no líquido cefalorraquidiano, respetivamente. A agregação da transtirretina está relacionada com a amiloidose sistémica senil, a cardiomiopatia amilóide familiar, a polineuropatia amilóide familiar e a amiloidose familiar leptomeningeal. Atualmente, a terapia principal para estas amiloidoses é o transplante de fígado ou o transplante combinado de fígado e coração. Contudo, existem muitos problemas associados a esta estratégia, entre eles o facto de não ser uma opção viável para a amiloidose familiar leptomenigneal. Uma abordagem que tem vindo a ganhar força baseia-se na estabilização cinética da proteína nativa, dado que a dissociação do tetrâmero é o passo limitante na agregação da transtirretina. Num estudo recente, propusemos a utilização de tolcapone, um fármaco aprovado pela *United States Food and Drug Administration* para a doença de Parkinson, como um potente inibidor de agregação da transtirretina. Notavelmente, o tolcapone pode atravessar a barreira hematoencefálica e, por essa razão, pode tornar-se no primeiro tratamento farmacológico disponível para a amiloidose familiar leptomeningeal, uma forma rara de amiloidose de transtirretina, que afeta o Sistema Nervoso Central. Para explorar esta hipótese, utilizámos quatro variantes de transtirretina associadas com esta doença, A25T, L12P, V30G e Y114C. Caraterizámo-las em detalhe e fomos capazes de avaliar a atividade do tolcapone para todas elas. Observamos que estas variantes são extremamente instáveis e que afetam a estrutura quaternária da proteína de modo diferente. Ainda assim, demonstrámos que o tolcapone pode ligar-se com elevada afinidade a estas quatro proteínas e estabelece interações semelhantes às observadas para a proteína WT. É de realçar que obtivemos evidências que o tolcapone pode estabilizar estas variantes, prevenindo a agregação, desde que a estrutura quaternária não esteja completamente perdida. Os resultados deste estudo enfatizam o enorme potencial do tolcapone, que parece ser a única opção para pacientes com amiloidose familiar leptomeningeal, pelo menos neste momento. Adicionalmente, os aspetos que diferenciam o tolcapone dos outros inibidores, tornando-o num fármaco tão poderoso para as amiloidoses de transtirretina, apoiam o uso do tolcapone como base para redesenhar derivados ainda mais eficazes.

Palavras-chave: agregação de proteínas, amiloidoses de transtirretina, amiloidose familiar leptomeningeal, reposicionamento de fármacos, tolcapone, estabilização cinética, estratégia terapêutica.

IV. Table of contents

V. List of figures and tables

VI. List of abbreviations

AD – Alzheimer's disease
αsyn – α-synuclein
Aβ – Amyloid β-peptide
BBB – Blood-brain barrier
CD – Circular dichroism
CSF – Cerebrospinal fluid
DMSO – Dimethylsulphoxide
DTT - Dithiothreitol
EC_{50} – Half-maximal effective concentration
ER – Endoplasmic reticulum
FAP – Familial amyloid polyneuropathy
HBPs – Halogen binding pockets
LB – Luria Bertani
MAPK – Mitogen-activated protein kinase
MKPs – MAP phosphatases
M – TTR – Monomeric TTR
NSAID – Non-steroidal anti-inflammatory drug
OLT – Orthotopic liver transplantation
ON - Overnight
PBS – Phosphate buffered saline
PD – Parkinson's disease
RT – Room temperature
SAC – Senile amyloid cardiomyopathy
SSA – Senile systemic amyloidosis
T_4 – Thyroxine
ThT – Thioflavin-T
TTR – Transthyretin
WT – Wild-type

1. Introduction

1.1 Transthyretin

Transthyretin (TTR), which was initially called prealbumin, is one of the proteins responsible for the transport and delivery of thyroxine (T_4) to cells, in humans, as well as retinol (vitamin A). While T_4 binds directly to TTR, retinol does it through the formation of a complex with retinol binding protein [1,2]. In plasma, albumin and thyroid binding globulin compete with TTR for the binding of T_4 and, the fact that they have a higher concentration and/or present a higher affinity for this hormone, makes that TTR only transports around 15% of the total T_4 [3]. On the contrary, in the cerebrospinal fluid (CSF), TTR is the main transporter of T_4 [4]. After detection of TTR mRNA expression in the epithelial cells from the choroid plexus of all mammals, birds and reptiles and observation that this protein is secreted predominantly to the CSF and not to the blood, it was postulated that TTR found in the CSF derives mostly from the choroid plexus [5,6]. On the other hand, TTR circulating in the plasma is produced primarily in the liver [7].

Native TTR is a tetramer comprising identical subunits, each with 127 amino acid residues, with a molecular weight of approximately 55 kDa (Fig.1). TTR has a very high β-sheet content with only one small α-helical segment, formed by residues 75 to 83. Much of the chain (45% of the amino acid residues) is arranged in eight extended β-strands, labelled A to H, connected by loops with various lengths. In turn, these strands are organized into two β-sheets, spaced about 10 Å apart, one formed by the strands DAGH and the other by the strands CBEF. All the interactions between strands are antiparallel, with exception of the one between strands A and G that is parallel [8,9]. The association of two monomers into a dimer involves the establishment of different interactions between the β-strands H and F in one monomer and the equivalent strands H' and F' in the other monomer. These interactions are mainly hydrogen bonds, but also water bridged or hydrophobic interactions. Even though the dimers associate in the tetramer by opposing equivalent eight-stranded sheets (DAGHH'G'A'D') face-to-face in the center of the molecule, there is almost no interaction between these sheets. In fact, the main source of contacts is the AB loop that, at the same time, act as a spacer, keeping the sheets out of contact. In the tetramer, the AB loops of monomers A and C, and B and D, are positioned in two close pairs at each edge of the opposed sheets. The residues in the GH loops, which are located in the same position, also contribute for the

dimer-dimer contacts. The dimer-dimer interface involves all four monomers and is stabilized by both hydrophilic and hydrophobic interactions [9].

This interface creates two identical funnel-shaped T_4 - binding sites located in opposite sides of the molecule, which run in parallel to the *z*-axis [8].

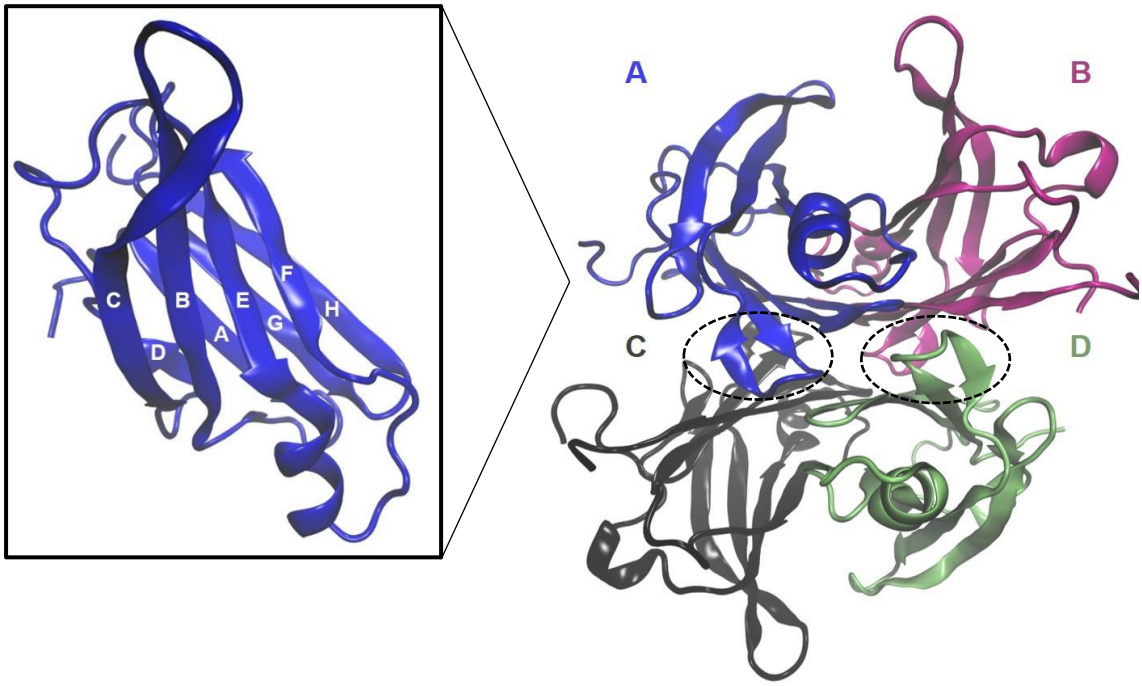

Figure 1. TTR structure. Cartoon representation of the WT protein (PDB: 1RLB). The subunits that compose the tetramer are depicted in different colors. The subunit A is enlarged to show the strands that form each monomer. The T_4-binding sites are surrounded by circles.

Although these sites are structurally equivalent, the association constants for T_4 differ in two orders of magnitude [10]. The existence of a high-affinity and low-affinity site is explained by a mechanism of negative cooperativity. Briefly, binding of the first hormone molecule in the primary site induces conformational changes that propagate to the secondary site through the network of hydrogen bonds. When the molecule binds to the second site, there are also changes in the primary site. However, the fact that the primary site is already occupied by the ligand protects it from major conformational changes and that is why the second ligand is less tightly bound [11].

In terms of amino acid composition, we can distinguish three groups that are arranged linearly along the binding pocket, which reading from the center are (Fig.2): (1) a hydrophilic patch formed by the hydroxyl groups of Ser 117 and Thr 119 and associated bound water molecules; (2) a hydrophobic patch formed by the methyl groups of Leu 17, Thr 106, Ala 108, Leu 110 and Val 121; (3) a group of charged residues such as Lys 15, Glu 54 and His 56. The side chains of Leu 110, Ser 115 and Ser 117 cause a constriction and narrowing of the channel near the mid-point (diameter of 4 instead of 8 Å) that defines an inner and outer binding cavity [12].T_4 fits into the binding pocket in such a way

that all its substituents establish favorable interactions with the residues mentioned. Namely, each of the 3' and 5'- iodine atoms contact with the side chains of Leu 17 and Leu 110 and each of the 3,5-iodines fits into a pocket lined with the methyl groups of Thr 106, Ala 108 and Val 121 and the methylenes of Lys 15 [12,13]. For this reason, the three pairs of symmetric hydrophobic depressions distributed throughout the channel are referred to as the halogen binding pockets (HBPs) (Fig.3) [9,14]. Besides the interactions established by the iodines, the 4' hydroxyl group interacts with the hydroxyl groups of Ser 117 and Thr 119, via a water molecule, and the α-carboxylate and α-amino groups with Lys 15 and Glu 54, respectively [12,13]. This mode of binding is normally referred as the forward mode, but it is probable that the hormone can also bind in the reverse mode, in which the α-carboxylate is oriented towards the inner binding pocket. A combination of forward and reverse mode has been observed for triiodothyronine, another thyroid hormone, and for bromoflavones, which compete with thyroid hormones for binding to TTR [15,16].

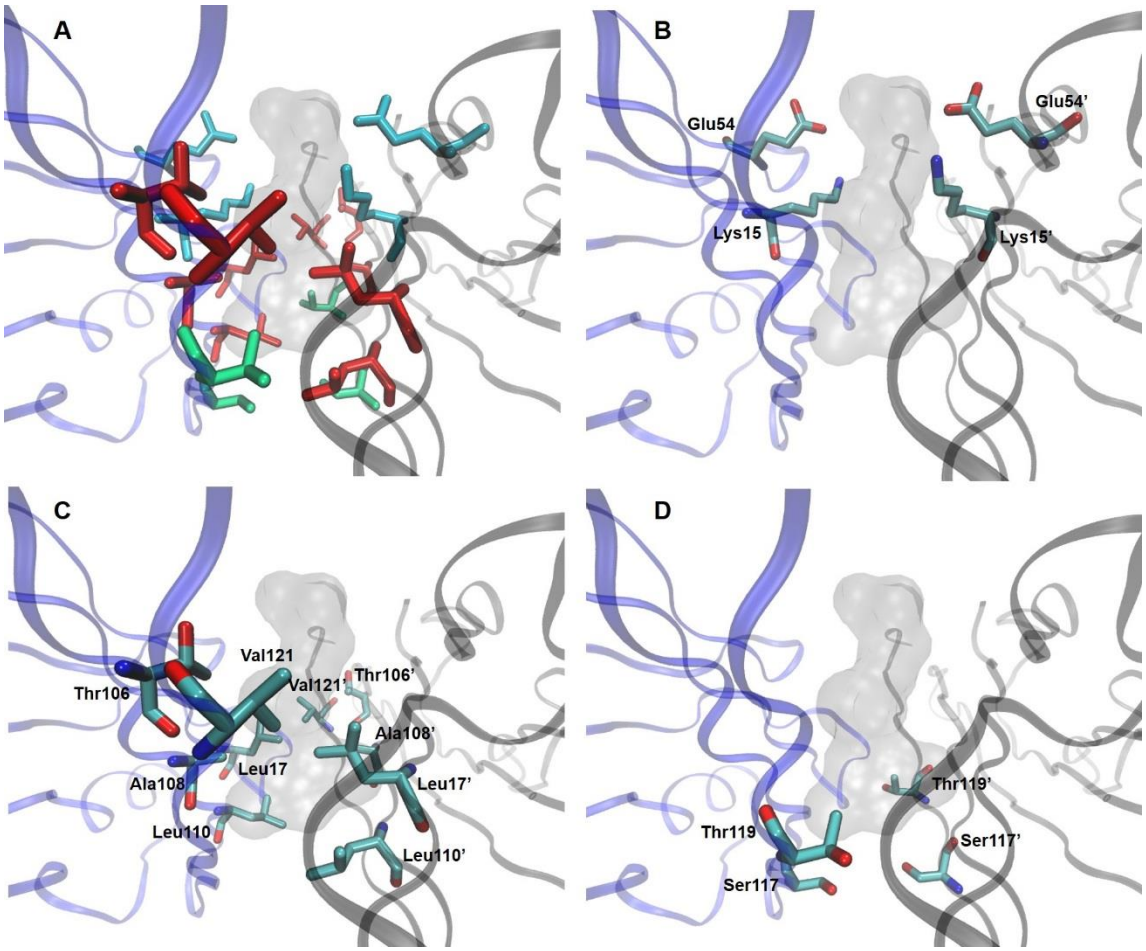

Figure 2. **T_4 – binding pocket.** Illustration of the residues present on the channel formed by the chains A (blue) and C (black). In (A) it is possible to see the position of the three groups of residues that compose the channel: charged residues (blue), hydrophobic residues (red) and hydrophilic residues (green). The residues that form each of these patches are shown in B, C, D, respectively. The space occupied by the ligand is shown in Surf. Structure prepared from the crystallography structure 2ROX.

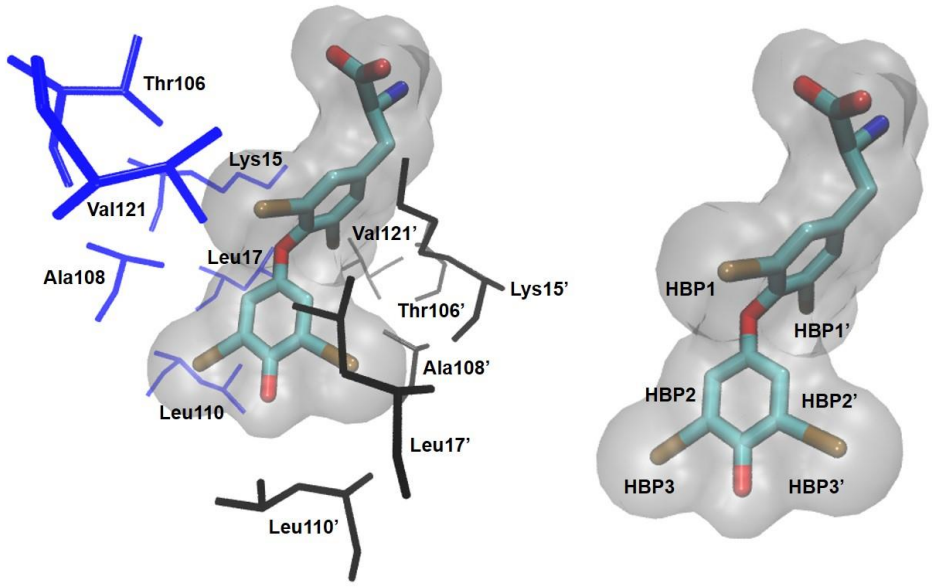

Figure 3. **TTR residues involved in T_4 binding**. Representation of the residues that interact with the iodine atoms (in brown) of T_4. The hormone is exhibited in grey translucent surface, putting in evidence the HBPs. Structure prepared from the crystallography structure 2ROX.

1.2 Transthyretin-related amyloidosis

The classical definition for amyloidosis states that it is a group of diseases characterized by the extracellular accumulation of amyloid fibrils, highly organized structures that arise from the misfolding and subsequent aggregation of proteins [17]. TTR is one of the proteins that were shown to form fibrils *in vivo*. Other examples include amyloid β peptide (Aβ) and α-synuclein (αsyn), which are associated with Alzheimer's disease (AD) and Parkinson's disease (PD), respectively [18].

TTR aggregation is linked to senile systemic amyloidosis (SSA), familial amyloid cardiomyopathy (FAC), familial amyloid polyneuropathy (FAP) and the familial leptomeningeal amyloidosis [19–25].

SSA is a sporadic disease caused by the aggregation and deposition of TTR wild-type (WT), preferentially in the myocardium (cardiomyopathy). This deposition leads to a progressive increase of the ventricular wall thickness that, in turn, results in a congestive heart failure and, ultimately, death. SSA is a late onset disease and it is quite common, as it affects as much as 25% of the population over 80 years old, especially men [21,26,27].

On the other hand, FAC, which is clinically similar to SSA, is associated with the accumulation of mutant TTR and follows an autosomal dominant inheritance pattern, meaning that only one mutated allele (of the gene codifying for the variant protein) is enough to be affected by the disorder [20,27] The most common mutation linked to FAC is

a single amino acid substitution of isoleucine for valine at position 122 (V122I), it was discovered in 1988, in fibrils isolated from a 68-year old black man. In fact, this mutation is almost exclusively encountered in patients of African origin. In the USA, which has the highest number of cases described, the occurrence of cardiac amyloidosis after the age of 60 is four times more common among the black in comparison to the caucasian population and the TTR V122I variant is responsible for approximately 25% of these cases [20,27,28].

In resemblance to FAC, FAP is caused by the expression of TTR variants and it is a dominantly inherited disease. FAP was first described in Portugal, in 1952, by Dr. Corino de Andrade, and was subsequently reported in Japan and Sweden. Although cardiac involvement is reported in several cases of FAP, it is typically characterized by a sensory-motor deficit and autonomic dysfunction. The polyneuropathy generally starts in the lower extremities and it includes the loss of voluntary movement and the impairment of thermal and painful sensitivity. As larger sensory and motor nerve fibers become affected, the patients start to have difficulties on walking, requiring walking aids and, eventually, a wheelchair. Regarding the autonomic dysfunction, orthostatic hypotension, episodes of diarrhea and constipation, and erectile dysfunction, in men, are the most common manifestations. This clinical profile corresponds to the so-called type I FAP, or Portuguese type, and is similar among the patients in Portugal, Japan and Sweden. However, in Sweden, there is a higher age at onset (50-60 years old) than in Portugal and Japan (30-40 years old) and the disease seems to progress more slowly [29–31]. The analysis of TTR isolated from patients with FAP revealed the presence of a methionine residue at position 30, instead of a valine (V30M) [32]. Despite more than 100 mutations have been related to FAP, the V30M substitution is the predominant genetic cause in the regions where the disease is endemic, like Portugal and Sweden, meaning that it is localized to a small area, with a traceable family history. In non-endemic areas, the disease is mainly sporadic, with genetic heterogeneity [33] (Fig. 4).

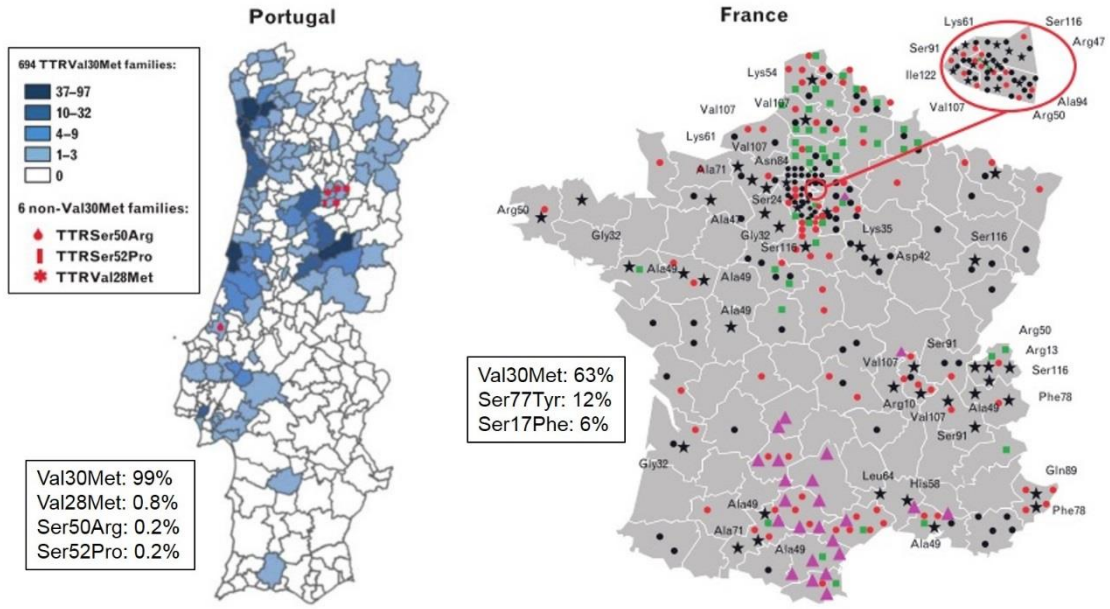

Figure 4. Location of TTR genotypes in Portugal (endemic area) and France (non-endemic area). Although the most common mutation in both countries is V30M, various mutations have been linked to FAP in France, on the contrary of Portugal. The prevalence of the three most common mutations for each country is indicated. Figure adapted from Parman *et al*. [33].

Finally, familial leptomeningeal amyloidosis, is an inherited disease and a rare type of TTR amyloidosis since its main feature is the impairment of the Central Nervous System (CNS). In this disease, the amyloid deposits are found in the leptomeninges, which is the designation given to the pia mater and arachnoid together, and in the subarachnoid vessels. Patients with this pathology present recurrent subarachnoid hemorrhage, raised protein level on the CSF, seizures and progressive cognitive impairment with dementia [22–25]. When this is associated with amyloid deposits in the vitreous humor, it is known as familial oculoleptomeningeal amyloidosis [22–24,26]. Additionally, the patients may manifest symptoms typical of FAP, depending on which is the TTR variant behind the disease [22–26,34]. Very few mutations have been related to leptomeningeal amyloidosis, from which the TTR variants A25T [25,35], L12P [36], V30G [37] and Y114C [24] are highlighted here, as they were the focus of this work (Table 1).

Table 1. Phenotype reported for TTR mutants A25T, L12P, V30G and Y114C.

Mutation	CNS amyloidosis	Vitreous opacities	Polineuropathy	Autonomic neuropathy	Heart amyloidosis
A25T	x	-	x	-	-
L12P	x	x	x	x	x
V30G	x	x	-	-	-
Y114C	x	x	x	x	x

1.3 Transthyretin aggregation mechanism

Understanding the mechanism by which a soluble protein is transformed into fibrils is crucial to design therapeutic strategies. In the case of TTR, the most accepted theory is that the tetramer first dissociates and then the natively folded monomer experiments slight tertiary structural changes to become aggregation competent (Fig. 5) [38–40].

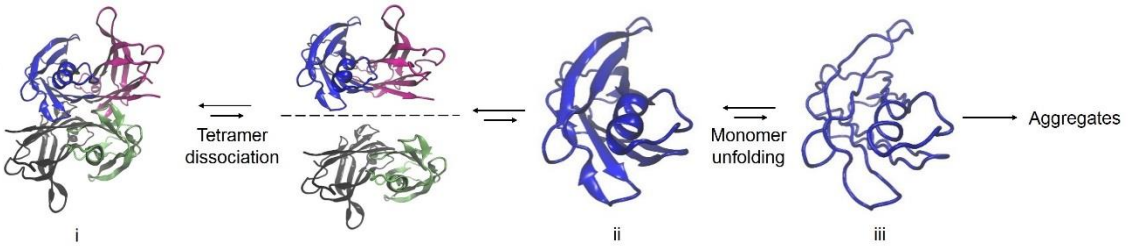

Figure 5. TTR aggregation mechanism. The proposed mechanism for TTR aggregation defends that the tetramer (i) dissociates into dimers that readily convert into monomers (ii), which partially unfold, forming an amyloidogenic intermediate (iii). This intermediate finally gives origin to the aggregates.

Tetramer dissociation is the rate-limiting step in TTR aggregation and preventing it has been the focus of drug research [41–45]. From the possible mechanisms of dissociation, the most likely is that the scission occurs along the AB/CD dimer-dimer interface, as it is the weakest of the two interfaces in the tetramer, yielding two dimers that readily convert into monomers [40]. However, protein disassembly is not enough for triggering amyloid fibril formation, since native TTR monomers (M-TTR) are not amyloidogenic unless they are partially unfolded [46]. The observation that TTR amyloid fibrils could arise from a partially denatured intermediate was first made by the research group of Jeffrey Kelly in 1992. In this study, the authors demonstrated that the protein can assemble into fibrils by lowering the pH to a value between 4.8 and 3.6, which is found inside lysosomes [38], suggesting that these organelles are involved in human amyloid disease [47].

The same group studied further in detail the acid denaturation pathway of TTR to characterize the aggregation competent intermediate. They observed that over the pH range 5.0 – 3.5, TTR undergoes a tetramer to monomer transition that is associated with aggregation. On the contrary, at pH below 3.5, TTR is mainly monomeric but unable to form amyloid fibrils. The difference between the two types of monomers lies in the tertiary structure. From pH 5.0 to 3.5, the monomers maintain their secondary structure and most of the tertiary structure, as indicated by fluorescence spectroscopy, far- and near-UV circular dichroism (CD). Accordingly, the monomeric species formed at pH 4.4, where amyloid fibril formation is maximal, display minimal binding to 1-anilino-8-naphtlenesulfonate, meaning that they are not markedly hydrophobic. When the pH is

lowered below 4, the fluorescence intensity of 1-anilino-8-naphtlenesulfonate rises, suggesting an increase in the hydrophobic patches exposed. At the same time, the monomers begin to lose the native-like tertiary structure and, ultimately, adopt a molten globule-like acid-denatured state and they are not able to form aggregates. In summary, the amyloidogenic intermediate is a monomer with an altered, but defined, tertiary structure. Continuing with the intermediate characterization, the authors aimed at discovering which is the site where the tertiary structural rearrangements occur. For that purpose, they took advantage of the fact that TTR has only two tryptophan residues, which are far apart in the native tertiary structure, and created two variants containing one single tryptophan residue (W41F and W79F). In this way, the profile of the fluorescence denaturation curves relies on only one residue and the changes happening in the TTR region nearby. They observed that the curve derived from the tryptophan residue 41 (W79F-TTR) is the main responsible for the curve exhibited by TTR WT, which suggests that the structural changes take place in the C-strand-loop-D-strand region of TTR [39].

After formation of the amyloidogenic intermediate, TTR aggregation is a downhill polymerization, meaning that the amyloidogenic monomer is the highest energy specie in the reaction. In other words, all the steps along the pathway are thermodynamically favorable and there is no kinetic barrier to oligomerization (Fig. 6A) [48]. This behavior is very different from the one presented by many of the aggregation-prone proteins we know, which follow a nucleation-dependent polymerization. In this case, the process begins with the formation of a nucleus, which is the rate-limiting step of the reaction and takes place during the lag phase (Fig.6B). After fibrillation, fibril growth occurs rapidly (exponential phase), until the depletion of monomers leads to a rate decline and, ultimately, to the plateau phase. The lag phase is the one that sets the rate of fibrillation and it can be accelerated by adding preformed aggregates, the so-called seeding effect [18,49,50].On the contrary, TTR amyloidogenesis is not seedable, which is the clearest evidence that it is not nucleation-dependent [48]. Additionally, no lag-phase is observed when the reaction is monitored by Thioflavin-T (ThT), a fluorescent dye commonly used for *in situ* amyloid detection since it is highly specific for amyloid fibrils [48,51,52]. Also, there is an immediate variation of the signal detected by CD and tryptophan fluorescence, which indicates an increase in β-sheet conformation and the burial of tryptophan residues within aggregates, respectively [48,51]. The appearance of aggregates in early time points ($\leq$ 180 s for 0.2 mg/mL M-TTR) was confirmed both by Atomic Force Microscopy and Electron Microscopy [48]. These initial species seem to be soluble oligomers, constituted by 6 to 10 monomeric units, as assessed by size exclusion chromatography, that have the minimal structure required for ThT binding [48,51]. The accumulation of intermediate

oligomeric species in the path of TTR aggregation is not surprising since the growth of the oligomers into fibrillar aggregates is the slower step in the aggregation pathway, after tetramer dissociation [51]. As the aggregation proceeds, the peak corresponding to these oligomers increases and the elution volume decreases, pointing to a rise of both concentration and size of the aggregates. Eventually, this peak and the monomer peak disappear and there is only one that corresponds to large aggregates, which elute in shorter volumes or even in the exclusion volume of the column [48,51].

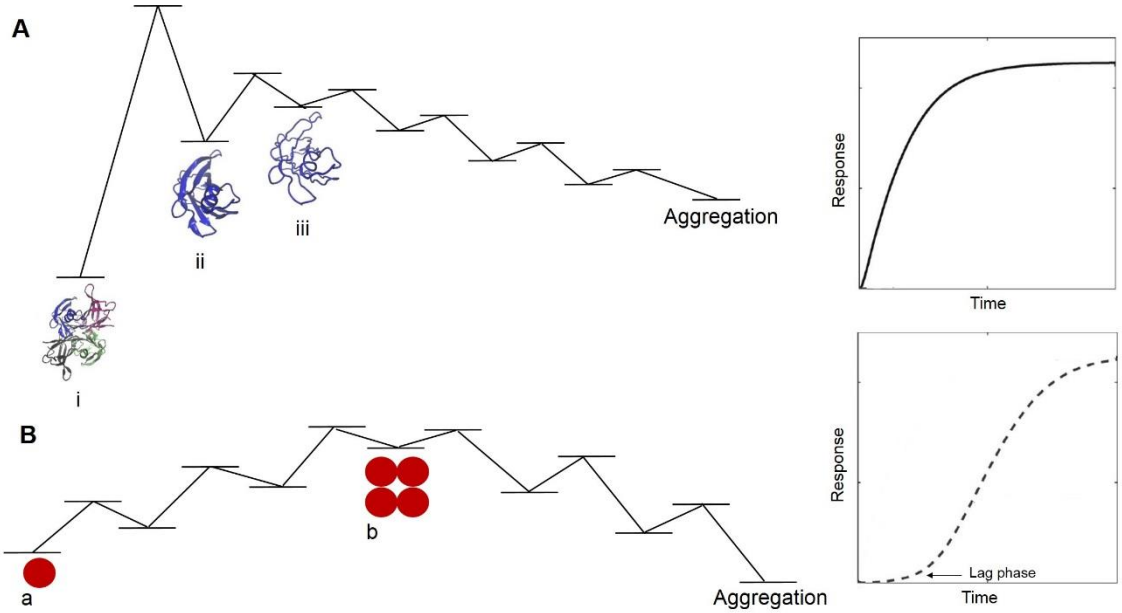

Figure 6. Downhill versus nucleated polymerization. Energy diagrams associated with downhill (A) and nucleated (B) polymerization. TTR aggregation involves the conversion of tetramers (i) into folded monomers (ii), which, in turn, unfold , forming an amyloidogenic intermediate (iii). After the intermediate is formed, all the steps that lead to aggregation are favourable. As a result, the curve that describes aggregation (on the right), when monitored for example with ThT, in function of time, fits to a hyperbolic curve. On the contrary, in a nucleated reaction, the first steps of aggregation involve the formation of a nucleus (b) from an unstructured monomer (a), through a series of unfavourable steps. In this case, the curve presents a lag phase that corresponds to nucleus formation and fits to a sigmoidal curve.

More recently, a different mechanism for TTR aggregation was proposed that does not depend on pH. This theory defends that TTR amyloidogenesis is triggered by proteolytic cleavage and it is supported by the fact that the amyloid deposits formed by the majority of TTR variants *in vivo* contain the truncated 49-127 polypeptide [53,54]. Although the protease responsible for this is not known, the authors used trypsin in their experiments and observed that it cleaves the 48-49 peptide bond of the S52P mutant. Nonetheless, the cleaved fragment 49-127 needs to be released from the protein to induce aggregation, which, *in vitro*, was achieved by increasing the shear stress. On the other hand, the shear stress itself enhances the susceptibility of TTR variants to proteolytic cleavage, meaning that variants that without shear stress did not experiment proteolytic

cleavage, are also affected. This was the case for the TTR variants L55P, V122I and V30M, and even TTR WT. Belloti and co-workers proposed that this mechanism could happen *in vivo*, especially in the heart, where the shear forces generated by fluid flow are particularly high [53].

1.4 Amyloidogenic potential of transthyretin variants

Much effort has been placed on trying to explain why some TTR variants are associated with disease while others are not, or even protect from it. This is particularly difficult as mutations were identified all over the sequence of the protein, with no tendency to accumulate in any specific part of the structure (Fig. 7).

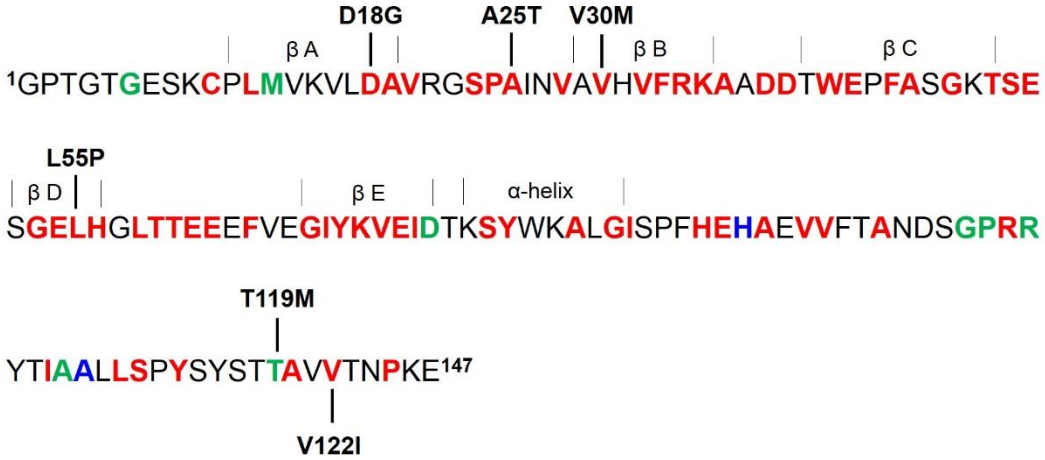

Figure 7. TTR sequence with sites of reported mutations. The mutations are equally distributed along the TTR structure. Most of the sites are associated with pathogenic mutations (red), but there are also non-pathogenic mutations (green) or sites where both cases were described (blue). Mutations referred in this chapter are pinpointed. The information used for this figure can be consulted in http://www.amyloidosismutations.com/mut-attr.php (accessed on 18.07.17).

Considering the structure of the different TTR variants, it is not possible to do this discrimination, as there are only minor structural changes between them. As a matter of fact, almost all variant structures crystallize in the same space group as the WT protein, $P2_12_12$, emphasizing that the overall structure is maintained [55]. An exception to this is the TTR variant L55P, which causes a very aggressive form of FAP and, interestingly, crystallizes in a different space group, C2, where the observed packing interactions are different from the other crystal structures, suggesting a potential important role on amyloid formation [56].

Another way of explaining the amyloidogenic potential of TTR variants is through the stability of tertiary and quaternary structures. Taking into account the aggregation mechanism proposed above, it is clear that high rates of tetramer dissociation and/or low

stability of the monomer are associated with increased amyloidogenic potential. Studying the equilibria of dissociation and of unfolding independently would be ideal, but at the concentration of TTR used in denaturation studies they are thermodynamically linked [57,58]. Nevertheless, it was possible to withdrawn some conclusions from the experiments performed. It was observed that TTR L55P dissociates 10-fold faster than TTR WT and that the monomers are highly destabilized, explaining why this mutation is so pathogenic and confers the earliest age of disease onset (second decade of life) [57,59]. Although the monomers of TTR V30M are equally destabilized to the ones of TTR L55P, the TTR V30M tetramers dissociate slightly slower than TTR WT tetramers and, consequently, the amyloidogenic intermediate cannot accumulate [57,58]. This can explain why TTR V30M disease phenotype is milder than the one of TTR L55P [57]. In fact, it appears that the rate of fibril formation is directly correlated with the rate of tetramer dissociation. Ordering the rates of fibril formation from the highest to the lowest gives L55P > V122I > WT > V30M > T119M, which is the same as for the dissociation rates. The TTR variant T119M has a dissociation half-life of 1534 hours (versus 42 hours for the WT protein, in the same conditions) and it forms fibrils 3000-fold slower than TTR WT [57]. Patients expressing both TTR T119M and TTR V30M (compound heterozygotes) develop a mild late-onset pathology, if at all, since the incorporation of TTR T119M subunits into TTR V30M homotetramers increases the kinetic barrier of tetramer dissociation. Consequently, the amyloidogenicity of the hybrid tetramers reduces and it is said that the TTR variant T119M acts as a *trans*-suppressor of amyloidosis [60].

Regarding the TTR variants associated with familial leptomeningeal amyloidosis, it seems that they have the lowest thermodynamic and kinetic stability [61]. This is particularly true for the TTR mutants A25T and D18G. Indeed, TTR A25T dissociates 1200-fold faster than TTR WT and 126-fold faster than TTR L55P, and TTR D18G is not even able to form tetramers. Therefore, one would expect that these variants originate a severe early-onset systemic amyloidosis, but this is not the case. Instead, CNS impairment is the main manifestation and it occurs around the fifth decade of life. The fact that patients with A25T and D18G mutations exhibit low or undetectable serum TTR concentration, respectively, suggests that this factor can protect the patient from an aggressive systemic disease. The authors proposed two possible explanations for this, one is that the variants are not efficiently secreted from the liver and the other is that they are rapidly degraded post secretion [62,63]. The secretion of these TTR mutants was studied in two cell lines, from kidney and liver, and, in both, the amount of secreted protein was markedly lower compared to the WT protein. For TTR DD18G, it appears that it is targeted for endoplasmic reticulum (ER) associated degradation. Interestingly, the fact that TTR D18G is largely monomeric does not explain its poor secretion since

the engineered M-TTR was secreted at 70% of the efficiency of TTR WT, which is higher than TTR A25T and TTR D18G [61]. The destabilization of TTR D18G tertiary structure compared to M-TTR by 3.1 kcal/mol is probably a better explanation for its poor secretion [63]. Sejkijima *et al*. (2005) explored the link between secretion efficiency and kinetic and thermodynamic stability of TTR variants and found that the combination of these two parameters dictates whether the protein is secreted. In detail, it appears that the ER associated degradation machinery detects mutants with a combined stability score below 0.8, above which the variants are secreted at maximal efficiency. In this way, the most destabilized variants will exist at a lower concentration in blood, what protects the carriers from a severe early onset amyloidosis [61]. On the contrary, a portion of these variants seem to escape to the quality control machinery in the choroid plexus, being secreted to the CSF [62,63]. Actually, the cells from the choroid plexus secrete TTR A25T as efficiently as TTR WT and in higher amount than the other cell lines [61]. It was hypothesized that the high T_4 concentration in the former tissue could chaperone these proteins, allowing their secretion. However, once in the CSF, the concentration of T_4 is insufficient to stabilize the proteins, which dissociate and misfold, forming amyloid deposits in the leptomeninges and subarachnoid space. Nevertheless, this CNS pathology manifests later in life, probably due to the low concentration of these TTR mutants in the CSF [61,63].

1.5 Mechanism of neurotoxicity

For several years, the neurological damage in protein-misfolding diseases was attributed to amyloid fibrils, but, in the recent years, accumulating evidence suggests that the lower-molecular-mass species are the most toxic. In PD, the new hypothesis claims that αsyn oligomers may be the most pathogenic species and that this is due to their ability to penetrate cellular membranes and, in some cases, to form pores -, despite this has never been observed *in vivo* [64,65].

Reixach *et al*. (2004) used a cell-viability assay to assess which are the cytotoxic species in TTR amyloidosis. The incubation of a neuroblastoma cell line with TTR amyloid fibrils and purified soluble aggregates (100 kDa or larger) was not toxic to the cells. On the contrary, monomeric TTR or small aggregates with the maximum size of 6 subunits, triggered apoptosis in the same cells [66]. One of the mechanisms proposed to explain TTR cytotoxicity is the disruption of cytoplasmic Ca^{2+} homeostasis. TTR induced an increase in the intracellular concentration of Ca^{2+} that results from an influx of extracellular Ca^{2+} across the plasma membrane, mainly via voltage-gated calcium channels. These channels are localized to specific lipid rafts within membranes and it

seems that TTR alters their organization, activating the channels. This dysregulation was maximal when TTR oligomers (< 100 nm diameter) were used, which supports the theory that oligomers, rather than mature fibrils, are the major cytotoxic species [67].

Additionally, TTR deposits seem to interfere with the ER stress response, which is normally activated by cellular stress conditions, such as altered redox status and expression of misfolded proteins. TTR oligomers can trigger this response and this is mediated by the release of Ca^{2+} from ER stores. This response involves, between other effects, the activation of caspase-3 and, subsequently, cell death [68].

Another pathway that appears to be altered by TTR is the mitogen-activated protein kinase (MAPK) signaling. The MAPKs cascades are regulated by the MAP phosphatases (MKPs), which dephosphorylate and inactivate the MAPKs. In FAP, the expression of MKPs is down-regulated and, so, it is reasonable to think that the MAPKs cascades might be up-regulated. Indeed, there is an increase on MAPK 1/2 activation, which, in turn, phosphorylate and activate the ERK 1/2 kinases. The sustained activation of ERK 1/2 in the presence of TTR aggregates was demonstrated in a cell line that presents a phenotype like a Schwann cell, which are cells from the peripheral nervous system, and it was found to be mediated by the receptor for advanced glycation end-products. This activation seems to play an important role in the apoptosis stimulated by TTR aggregates since blocking ERK activation abolishes caspase-3 activation [69].

Other amyloid proteins, like Aβ, are known to affect similar biochemical pathways, which suggests that the amyloid conformation itself is toxic and that toxicity does not depend on the protein [69,70].

1.6 The kinetic stabilizer strategy

Currently, the main therapy for TTR amyloidosis is orthotopic liver transplantation (OLT), since the liver is the major source of plasma variant TTR. The first OLT was done in two Swedish patients with type I FAP and practically abolished the TTR V30M in circulation, which is replaced by the donor TTR WT [71]. The follow-up of four patients during the first two years after surgery revealed that, with exception of one patient, there was a general improvement of the autonomic symptoms, the neurological decline was halted and there was a decrease of amyloid deposits [72]. The results from ten years of experience with OLT collected by the Familial Amyloidotic Polyneuropathy World Transplant Registry indicate that approximately 60 OLTs are performed annually worldwide and most of them on patients with the V30M mutation. From the cases analyzed, it appears that there is an improvement of the neurological, nutritional and, especially, gastrointestinal

manifestations. Oppositely, the cardiovascular involvement does not seem to improve and, indeed, most of the deaths are related to it. Finally, they found a significant increase in the 5-year patient survival for patients with the V30M mutation (79%), which was not observed for patients with other mutations (56%) [73]. This difference was attributed to the progression of the cardiomyopathy in some of these patients that is probably caused by deposition of the WT protein, prompted by a template of TTR amyloid [74]. For this reason, FAP patients that present cardiac amyloidosis before the transplant have a higher risk of dying and it should be considered a combined liver and heart transplant [28,73]. While not so evident, signs of cardiomyopathy related with TTR WT have also been described in patients with the V30M mutation. As a factor that limits survival, combined liver and heart transplantation might also be an option for this variant [28,73,75].However, neuropathy can still advance in patients after having the surgery, for the same reason as for cardiomyopathy. Moreover, the peripheral nerve amyloid deposition may derive from the TTR synthetized in the choroid plexus, which is transmitted from the CSF to the peripheral nerves [76].

For patients with FAC, combined heart and liver transplant has been employed, and for SSA, only heart transplant, since it is related with TTR WT [28,73].

In conclusion, there are several problems associated with these treatments: (1) cardiomyopathy and neuropathy can advance due to the aggregation of the WT protein; (2) liver transplantation does not replace the variant TTR that is produced on the choroid plexus, meaning that it is not a viable option for leptomeningeal amyloidosis; (3) liver and/or heart transplants require life-long immunosuppression that makes the patient more susceptible to other diseases. Hence, there is a huge need for finding other strategies to ameliorate TTR-related amyloidosis.

One approach that has been gaining power is based on the kinetic stabilization of native TTR. It started with the observation that raising the kinetic barrier of tetramer dissociation by incorporation of TTR T119M subunits into a tetramer composed of disease-associated subunits protects from disease [60]. This stabilization may result from the establishment of new contacts between both monomers in one dimer and between the two dimers [77]. Therefore, researchers hypothesized that small molecules that can bind to one or both T_4 - binding sites should stabilize the AB/CD dimer-dimer interface by interacting with the A and C and/or B and D subunits [78]. The first evidence came from the demonstration that T_4 inhibits TTR amyloid fibril formation *in vitro* and triggered an intensive search for molecules that bind with high affinity to the thyroxine binding sites [79]. Most of these molecules were created through structure-based drug design and screening, based on TTR/(small molecule)$_2$ co-crystal structures [14]. Typically, the small molecule TTR ligands have two aromatic rings, which can be directly linked or separated by hydrophobic linkers

of variable chemical structure (Fig.8). Normally, one aromatic ring is substituted with a polar substituent and the other ring presents halogenated substituents, alkyl groups, or a combination of both [14,78]. Although some ligands bind to TTR in the reverse mode, the most favorable interactions are achieved when these molecules bind in the forward mode. In this way, the polar substituents can make important electrostatic interactions with Lys15/15' and, possibly, with Glu54/54', on the periphery of the outer binding site and/or engage in complementary hydrophobic interactions with the HBPs 1/1' and/or 2/2'. Concurrently, the halogenated or alkylated rings, which occupy the inner binding cavity, can form hydrogen bonds with Ser117/117' or Thr119/119' and/or occupy the HBPs 2/2' and/or 3/3'. In case there is a linker, whether the compound binds in the forward or reverse orientation, it is positioned in the hydrophobic environment of HBPs 2/2' [41,57,78]. All the interactions between the ligand and TTR contribute to stabilize the tetrameric form of the protein, making the barrier for dissociation so high that the process becomes extremely slow under physiological conditions [42,57,78]. There are other important characteristics to be considered when designing a kinetic stabilizer. Namely, they must exhibit high binding affinity and high binding selectivity, they must not interact with the thyroid hormone receptor and they should exhibit minimal nonsteroidal anti-inflammatory drug (NSAID) activity as cyclooxygenase inhibition could worsen the renal, cardiac and gastrointestinal problems often presented by patients with TTR amyloidosis [41,78,80].

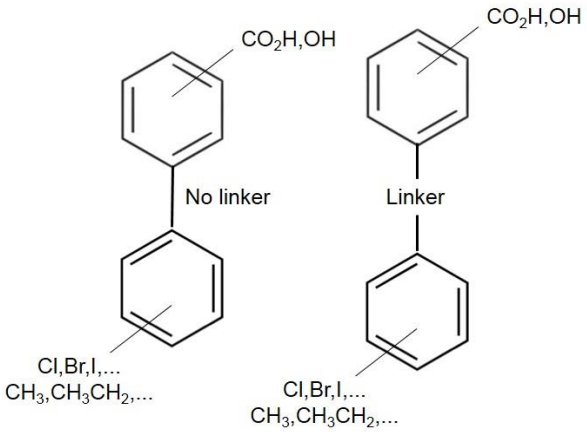

Figure 8. General structure of the TTR kinetic stabilizers. Examples of substituents that can replace the hydrogen atoms on the aromatic rings are depicted.

From the many TTR kinetic stabilizers that were identified, only three have reached human clinical trials until now (Fig. 9).

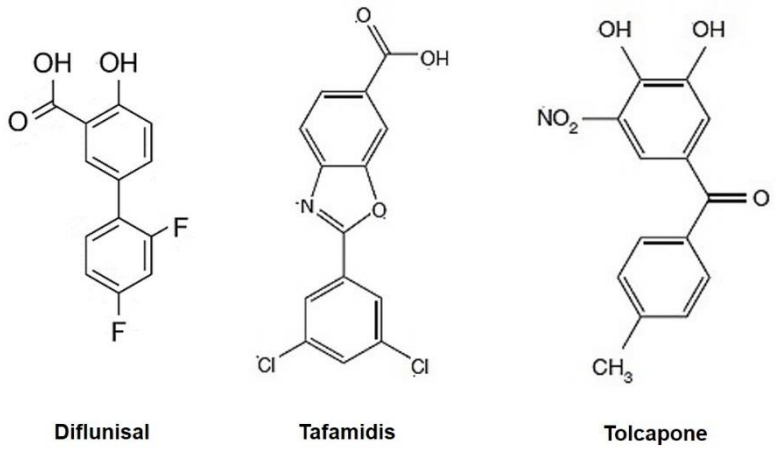

Figure 9. Diflunisal, tafamidis and tolcapone structure. The structure of these compounds is in agreement with the one illustrated in figure 6. Tolcapone structure gives the example of a compound where the two rings are connected by a linker.

The first one is diflunisal, a NSAID approved by the United States Food and Drug Administration (FDA), which binds to TTR with negative cooperativity (K_{d1} = 75 nM, K_{d2} = 1.1 μM). *In vitro*, it was observed that diflunisal (at a therapeutic concentration) stabilizes TTR, protecting against urea- and acid-mediated denaturation [45,81]. These observations were confirmed *in vivo*, after oral administration of diflunisal in healthy subjects [81]. More importantly, the administration of diflunisal for 2 years compared with placebo slowed the progression of polyneuropathy and improved the quality of life for patients with FAP [82]. In conclusion, diflunisal could be effective for SSA, FAC and FAP, as it binds both TTR WT and clinically important variants. Other advantage is that it is already approved by drug agencies and has a known safety profile, since it is used for decades. However, even though TTR amyloidogenesis inhibition by diflunisal is mediated by a different mechanism than its anti-inflammatory activity, this could increase the susceptibility to develop renal impairment, heart failure and peptic ulceration, as mentioned before [45]. Furthermore, diflunisal may be ineffective against familial leptomeningeal amyloidosis because it cannot cross the blood-brain barrier (BBB) [83].

Another small molecule that supports the native state stabilizer strategy is the benzoxazole tafamidis, which was discovered by Kelly's group and developed by FoldRx Pharmaceuticals (acquired by Pfizer). Tafamidis was shown to bind with high selectivity, high affinity and negative cooperativity (K_{d1} ~ 2 nM and K_{d2} ~ 200 nM) to recombinant TTR WT. Consequently, tafamidis stabilizes the protein under fibril-promoting and denaturing conditions, but also under physiological conditions. Importantly, tafamidis binds with high selectivity to TTR in human plasma and kinetically stabilizes it in samples obtained from patients harboring a broad spectrum of TTR variants, including TTR V30M TTR and TTR V122I, or even from healthy volunteers (TTR WT homotetramers) [43]. This

stabilization was observed *in vivo,* in patients with early-stage V30M-FAP, after oral administration of tafamidis. This was associated with a reduction in neurological deterioration, preservation of nerve function, improved nutritional status and maintained quality of life [84]. The treatment with tafamidis was also beneficial for patients with non-V30M mutations, older and with more severe disease [85]. Regarding adverse events, none of the studies found major safety concerns associated with this drug [84–86]. The clinical benefits related to tafamidis, along with its low toxicity and the lack of NSAID activity led to its approval by the European Medicines Agency for the treatment of early-stage FAP[a]. However, this drug was not approved by the FDA, which required more studies to demonstrate its efficacy. Another drawback is that there are no evidences that tafamidis can cross the BBB and, therefore, is unlikely that CNS manifestations of TTR amyloidosis could be treated with this compound.

More recently, the group of Prof. Ventura, working together with SOM Biotech, identified another inhibitor of TTR amyloidogenesis, tolcapone. As for diflunisal, tolcapone was discovered by a strategy of drug repositioning [44]. Drug repositioning consists in giving a new use to compounds already licensed for a different therapeutic indication. These drugs have passed clinical trials, where the adverse events were assessed, and have, many times, phase IV (post-marketing surveillance) safety data. This reduces the cost and the time required to bring them to trial and into the clinic for their new application [87]. Tolcapone is a nitrocatechol and a potent inhibitor of catechol-*O*-methyltransferase, an enzyme involved in the catabolism of levodopa, which is the standard therapy for patients with PD. It inhibits both peripheral and CNS catechol-*O*-methyltransferase, increasing the amount of levodopa available for transport to the brain and the amount of levodopa and, consequently, dopamine, in the brain itself. The use of tolcapone as an adjunct to levodopa and carbidopa for the treatment of PD is authorized in the EU and USA [88,89]. *In vitro,* tolcapone binds with high affinity to TTR and inhibits very effectively, more than tafamidis, the aggregation of TTR WT and TTR variant V122I . Since tolcapone can cross the BBB, the authors tested whether it could reduce the aggregation of the leptomeningeal-associated variant, TTR A25T, and verified that it can. For the WT protein, this effect is mediated through tetramer stabilization, as tolcapone protected the tetramer from unfolding in the presence of 6.5 M urea, in a dose-dependent manner. Tolcapone's stabilizing effect protected from TTR cytotoxicity in FAC and FAP cellular model systems. Furthermore, it was observed that tolcapone binds and stabilizes TTR *ex vivo* in human plasma from WT and V30M individuals. This was confirmed *in vivo,* in plasma from transgenic mice expressing human TTR V30M, after oral administration of

[a] See www.ema.europa.eu for more details.

the drug and, more importantly, in human healthy volunteers (TTR WT). The structural data obtained for TTR WT and TTR V122I with tolcapone revealed the formation of more polar contacts and hydrophobic interactions than in the case of tafamidis [44]. As a result, tolcapone displays a similar affinity for the first binding site, but a much higher affinity for the second biding site than tafamidis, which may underlie why it is more efficient. A preliminary, open label, phase IIa clinical trial was conducted in patients with FAP at different stages, healthy individuals and asymptomatic carriers with mutations in the TTR genes. Treatment with a single oral dose of 200 mg or three doses of 100 mg of tolcapone stabilized plasmatic TTR in all patients studied and no adverse events were registered. In particular, no signs of hepatotoxicity, which has been previously related to tolcapone, were detected [88–90].

These results support further development of tolcapone for the treatment of different forms of TTR amyloidosis, including the ones that cannot be addressed with the current therapies.

Based on the preliminary results obtained with TTR A25T [44], we have conducted the present study aimed at validating whether tolcapone can become the first small-molecule treatment available for familial leptomeningeal amyloidosis. We have produced the more relevant mutants related with this pathology and characterized in detail the role of tolcapone in these proteins, demonstrating that tolcapone can become a broad-spectrum drug to treat TTR-related amyloidosis. Furthermore, the knowledge we have accumulated in this study led us to open a research line, which we are planning to develop in the near future, centered on the use of tolcapone to create rationally designed optimized derivatives.

2. Aims

Considering the preliminary results obtained with TTR A5T, we intended to explore the interaction and effect of tolcapone over this variant, as well as on other variants related with familial leptomeningeal amyloidosis, namely TTR L12P, TTR V30G and TTR Y114C. Importantly, the diseases caused by these TTR variants cannot be addressed with the current therapy for TTR amyloidosis.
Our main goals were:

1. To clone and produce the TTR variants A25T, L12P, V30G and Y114C and study their stability and aggregation.
2. To assess the effect of tolcapone on the aggregation and stability of these TTR variants.
3. To determine the binding parameters that describe the interaction between tolcapone and the proteins.
4. To analyze the interactions that drive the binding of tolcapone to these mutants.
5. To develop optimized forms of tolcapone through rational redesign.

3. Materials and methods

All the reagents presented in this section were obtained from Sigma-Aldrich (Missouri,USA) and AppliChem (Darmstadt, Germany), unless otherwise stated.

3.1 Transthyretin expression and purification

The vectors coding for TTR variants were prepared by PCR-site directed mutagenesis using the QuickChange Lightning kit (Agilent technologies, Santa Clara, California, USA). pET28a vector (Novagen, Addgene, Cambridge, USA) encoding for the WT protein was used as a template. The TTR WT cDNA was cloned into this vector in such a way that the expressed protein does not have both 6xHis and T7 tags. Briefly, a Polymerase Chain Reaction was performed with the template and two synthetic oligonucleotide primers, both containing the desired mutation (Table 2). These primers anneal to the same sequence on opposite strands of the plasmid and the plasmid is amplified during the extension phase of the reaction by a DNA polymerase. In the end of the reaction the amplification products were subjected to a digestion with the *Dpn I* restriction enzyme in order to eliminate the methylated parental DNA. Finally, the *Dpn I*-treated DNA was transformed into BL 21 – (DE3) *E.coli* competent cells. An isolated transformed colony was used to inoculate 10 ml of Luria-Bertani (LB) medium supplemented with 50 $\mu g.ml^{-1}$ kanamycin and the culture was incubated overnight (ON) at 37ºC, in agitation. This ON culture was used to inoculate 1 L of LB medium with 50 $\mu g.ml^{-1}$ kanamycin. The culture was grown at 37ºC, under agitation. TTR expression was induced with 1 mM isopropyl β-D-thiogalactopyuranoside (Apollo Scientific Limited, Cheshire, UK) when the culture reached an optical density (at 600 nm) of 0.8. The expressing bacteria were incubated in the same conditions ON and harvested by centrifugation (9,820 *x g* for 10 minutes). The cells were resuspended in 100 ml of lysis buffer (20 mM Tris HCl, 500 mM NaCl, pH 7.5) Cell lysis was attained through a freeze-thaw cycle and sonication and the soluble fraction was recovered by centrifugation. The intracellular proteins were fractionated by ammonium sulphate precipitation. The TTR-containing fraction precipitated between 50 and 90% ammonium sulphate. The precipitate was solubilized in 10 ml of 25 mM Tris HCl, pH 8, and dyalised against the same buffer. The sample was filtered on a Puradisc 30 sterile syringe filter 0.45 μM pore size (Whatman, GE Healthcare, Buckinghamshire, England) and 1mM dithiothreitol

(DTT) (nzytech, Lisboa, Portugal) was added. It was loaded on a HiTrap Q HP column (GE Healthcare) and eluted with a linear gradient 0 – 0.5 M NaCl in 25 mM Tris HCl, pH 8. The protein was precipitated from TTR-enriched fractions and dissolved in a small volume of 25 mM Tris, 100 mM NaCl, pH 8. It was further purified by gel filtration chromatography on a HiLoad 26/600 Superdex 75 prep grade column (GE Healthcare) and eluted with 25 mM Tris, 100 mM NaCl. The purest fractions were combined and stored at -20ºC. Protein concentration was determined spectrophotometrically at 280 nm using an extinction coefficient of 77 600 M^{-1} cm^{-1}. The WT protein was expressed and purified in the same manner as the TTR variants.

Table 2. Cloning of TTR variants A25T, L12P, V30G and Y114C. For each protein, the mutated residue in the protein, as well as the nucleotides of the primers that give origin to the mutation, are highlighted in red.

WT	MGPTGTGESKCPLMVKVLDAVRGSPAINVAVHVFRKAADDTWEPFASGKTSESGELHGLTTE EEFVEGIYKVEIDTKSYWKALGISPFHEHAEVVFTANDSGPRRYTIAALLSPYSYSTTAVVTNPKE	
A25T	MGPTGTGESKCPLMVKVLDAVRGSP**T**INVAVHVFRKAADDTWEPFASGKTSESGELHGLTTE EEFVEGIYKVEIDTKSYWKALGISPFHEHAEVVFTANDSGPRRYTIAALLSPYSYSTTAVVTNPKE	
	Forward primer	5'-CTGTGCGTGGTTCTCCG**A**C**G**ATTAACGTTGCAGTGCA-3'
	Reverse primer	5'-TGCACTGCAACGTTAAT**C**G**T**CGGAGAACCACGCACAG-3'
L12P	MGPTGTGESKCP**L**MVKVLDAVRGSPAINVAVHVFRKAADDTWEPFASGKTSESGELHGLTTE EEFVEGIYKVEIDTKSYWKALGISPFHEHAEVVFTANDSGPRRYTIAALLSPYSYSTTAVVTNPKE	
	Forward primer	5'-TGAGTCCAAATGTCCGC**C**GATGGTGAAAGTTCTGG-3'
	Reverse primer	5'-CCAGAACTTTCACCATC**G**GCGGACATTTGGACTCA-3'
V30G	MGPTGTGESKCPLMVKVLDAVRGSPAINVA**G**HVFRKAADDTWEPFASGKTSESGELHGLTTE EEFVEGIYKVEIDTKSYWKALGISPFHEHAEVVFTANDSGPRRYTIAALLSPYSYSTTAVVTNPKE	
	Forward primer	5'-GGCAATTAACGTTGCAG**G**GCACGTATTCCGCAAAG-3'
	Reverse primer	5'-CTTTGCGGAATACGTGC**C**CTGCAACGTTAATTGCC-3'
Y114C	MGPTGTGESKCPLMVKVLDAVRGSPAINVAVHVFRKAADDTWEPFASGKTSESGELHGLTTE EEFVEGIYKVEIDTKSYWKALGISPFHEHAEVVFTANDSGPRRYTIAALLSP**C**SYSTTAVVTNPKE	
	Forward primer	5'-CGCTGCTGTCTCCGT**G**CTCTTACAGCACCAC-3'
	Reverse primer	5'-GTGGTGCTGTAAGAG**C**ACGGAGACAGCAGCG-3'

3.2 Transthyretin kinetic stability *in vitro*

TTR solutions (1.8 μM in phosphate buffered saline (PBS)) were incubated with 8 M urea at room temperature (RT) along time and the process of unfolding was tracked by intrinsic fluorescence spectroscopy, using a FP-8200 Spectrofluorometer (Jasco, Easton,USA). The samples were excited at 295 nm, allowing the selective excitation of the Trp residues on the protein, and fluorescence emission spectra were recorded from 310 to 400 nm. Upon denaturation, the Trp residues become more solvent-exposed and the maximum fluorescence changes from 335 nm to 355 nm, approximately. The

355/335 nm fluorescence emission intensity was used to follow TTR unfolding and plotted as a function of time. The curves were fitted to a single exponential function: $\text{Fluorescence intensity}^{355/335} = \text{Fluorescence intensity}_0^{355/335} + \left(\text{Plateau} - \text{Fluorescence intensity}_0^{355/335}\right) \times \left(1 - \exp^{(-k_{diss} \times t)}\right)$, where $\text{Fluorescence intensity}_0^{355/335}$ is the native protein fluorescence intensity ratio (355/335), k_{diss} is the tetramer dissociation rate constant and t is the time, in hours. The GraphPad Prism 6 software (GraphPad Software Inc., California, USA) was used for data analysis.

3.3 Transthyretin aggregation *in vitro* as a function of pH

A TTR stock solution (7.3 µM in 10 mM sodium phosphate, 100 mM KCl (Merck, New Jersey, USA), 1 mM EDTA, 1 mM DTT, pH 7.0) was diluted 1:1 with 100 mM acidification buffer, containing 100 mM KCl, 1 mM EDTA and 1 mM DTT. To attain pHs in the range 3.0-7.5, three acidification buffers were prepared: with citrate buffer (for pH 3.0), with acetate buffer (for pH 3.5-5.5) and with phosphate buffer (for pH 6.0-7.5). All samples (final concentration of 3.65 µM) were incubated for 72 hours at 37ºC and the aggregation was assessed by light scattering, with the excitation and emission wavelengths set at 340 nm, using a Varian Cary Eclipse Fluorescence Spectrophotomer (Agilent, Santa Clara, California,USA).

3.4 Transthyretin aggregation inhibition *in vitro*

TTR solutions (7 µM in 10 mM sodium phosphate, 100 mM KCl, 1mM EDTA, 1 mM DTT, pH 7.0) were incubated with varying concentrations of tolcapone (from 0 to 50 µM) for 30 minutes at 37ºC. Since the stock solutions of tolcapone were prepared in dimethyysulphoxide (DMSO), the percentage of DMSO in all the samples was adjusted to 5% (v/v). After the incubation period, the pH was dropped to 5.0 via dilution 1:1 with acidification buffer (100 mM sodium acetate, 100 mM KCl, 1 mM EDTA, 1 mM DTT, pH 5.0) and the samples were incubated for more 22 hours at 37ºC. For TTR WT and TTR Y114C, a pH of 4.2 and an incubation period of 72 hours were used instead. The formation of aggregates was evaluated as before. TTR aggregation was considered maximum in the absence of tolcapone (100% aggregation).

3.5 Urea denaturation curves in the absence or presence of tolcapone

Urea in 50 mM sodium phosphate, 100 mM KCl, pH 7.0, was added to a TTR stock solution (1 μM in PBS) to obtain a range of final concentration from 0 to 9.5 M, the samples incubated for 96 hours at RT. The concentration of urea in the solutions was verified by refractive index, using a Manual Hand-held Refractometer HR901 (A.Krüss Optronic, Germany). TTR unfolding was measured as explained before. The 355/335 nm fluorescence emission intensity was normalized from minimum (folded) to maximum (unfolded), and plotted as a function of urea concentration. For evaluating the effect of tolcapone in the stability of the proteins, the TTR solutions were incubated with 20 or 50 μM tolcapone (same percentage DMSO) instead. In this case, the curves with and without tolcapone were represented together and the 355/335 nm fluorescence emission intensity was normalized from minimum to maximum, with the maximum being the one of the control.

3.6 Urea-mediated transthyretin dissociation measured by resveratrol binding

TTR solutions (1.8 μM in PBS) were incubated with different concentrations of urea buffered with 50 mM sodium phosphate, 100 mM KCl, 1 mM EDTA and 1 mM DTT (pH 7.0) for 96 hours at RT. After this time, 1.8 μl of resveratrol from a 1 mM stock solution in DMSO was added to a 100 μl sample just before the measurement, in order not to shift the equilibrium towards the tetramer [57]. The incubation time with resveratrol was the same for all samples. The samples were excited at 320 nm and the fluorescence recorded from 350 to 550 nm. The fluorescence intensity at 394 nm was plotted as a function of urea concentration.

3.7 Isothermal titration calorimetry

The kinetic parameters that describe the interaction between TTR and tolcapone were determined by isothermal titration calorimetry (ITC), using a MicroCal Auto-iTC200 Calorimeter (Malvern Instruments Ltd, UK). The ITC and data analysis were done by the Dr. Adrián Velásquez-Campoy at BIFI-Zaragoza, as part of a collaboration between the

two groups. Briefly, TTR A25T or TTR Y114C at 5 μM located in the calorimetric cell was titrated against the compounds at 100 μM in the injection syringe in PBS buffer pH 7.0, 100 mM KCl, 1 mM EDTA, 2.5% DMSO, at 25ºC. A stirring speed of 1000 r.p.m. and 2 μl injections were programmed, with consecutive injections separated by 150 s to allow the calorimetric signal (thermal power) to return to baseline. For TTR L12P and TTR V30G the concentration of protein was increased to 20 μM, since the concentration of TTR able to bound tolcapone was low. For each protein, two replicates were performed and the experimental data was analysed with a general model for a protein with two ligand-binding sites [91,92] implemented in Origin 7.0 (OriginLab, Massachusetts, USA).

3.8 Crystal structures of Transthyretin/tolcapone complexes

Co-crystals of TTR A25T/tolcapone, TTR V30G/tolcapone and TTR Y114C/tolcapone were obtained at 18ºC by hanging drop vapor diffusion methods after mixing 115 μM (TTR A25T) or 85 μM (TTR V30G and TTR Y114C) protein with tenfold molar excess of tolcapone to ensure saturation. The reservoir solution contained PEG 400 (Jena Bioscience, Jena, Germany) (TTR A25T-25%; TTR V30G/Y114C-30%), 200 mM $CaCl_2$, HEPES 100 mM (pH 7.5 for TTR A25T and pH 7.0 for TTR V30G and TTR Y114C). Crystals appeared after one week incubation from equal amounts of protein solution (with tolcapone) and reservoir solution. Crystals were cryo-protected in reservoir buffer containing 10% glycerol and flash frozen in liquid nitrogen before diffraction analysis. Diffraction data was collected at the ALBA synchrotron in Barcelona (BL13-XALOC beamline) and the structures solved in collaboration with the Protein Structure group, directed by Dr. David Reverter, at our institute. All the structural representations in this thesis were prepared with the Visual Molecular Dynamics (VMD) 1.9.2 software (NIH Biomedical Research Center for Macromolecular Modeling and Bioinformatics, University of Illinois at Urbana-Champaign, USA). In all cases, the tetrameric assembly was created from the PDB with PDBePisa software (EMBL-EBI, Cambridgeshire, UK).

4. Results and discussion

We started by the characterization of the selected variants, in particular, by confirming the predicted structural alterations due to the mutations A25T, L12P, V30G and Y114C. The L12P and V30G mutations are situated in the β-strands A and B, respectively, while the A25T and Y114C are in the AB and GH loop, respectively (Fig. 10A). These loops are part of the dimer-dimer interface [9], suggesting that the TTR variants A25T and Y114C may have a higher impact on the structure. Moreover, the Y114C mutation is part of the monomer-monomer interface, which is maintained by the chains F and H of both monomers [9]. On the contrary, the L12P and V30G mutations are farther away from both interfaces (Fig. 10B).

In the case of TTR A25T, alanine, which is hydrophobic, is replaced by a polar residue, threonine. The side chain of threonine is bigger than the one of alanine, leading to a small movement of the C_α in the position 25, which is the main difference between the crystallographic structure of TTR A25T and TTR WT. Additionally, threonine is surrounded by hydrophobic residues with which it cannot interact, originating some disorder in this area [93]. Besides these effects, the tendency of threonine to form β-sheets can contribute to the amyloidogenicity of this variant. Alanine to threonine substitutions are found in many proteins that aggregate, like αsyn (A53T), and are known to influence protein stability and quaternary organization [94]. For TTR L12P, the hydrophobic leucine is substituted by a proline, which has a very rigid structure. This structure does not fit properly in β-sheet structures and that is why prolines are known as β-breakers [95]. In the TTR variant V30G, valine, which is also hydrophobic, gives place to glycine, which bears a single hydrogen atom in its side chain, occupying less space. Additionally, glycine gives more flexibility to the protein since it allows the residues to move freely, without the problem of steric hindrance. This flexibility disrupts the regularity of the backbone conformation required for the formation of a defined secondary structure, like α-helix or β-sheet [96]. Finally, in TTR Y114C, the type of amino acid residue is maintained, as both tyrosine and cysteine are polar. The biggest difference is that cysteine is smaller and is able to form a disulfide bound to a second cysteine through the very reactive SH group, as long as they are close enough. Indeed, the crystallographic structure of TTR Y114C revealed that it is similar to the one of TTR WT and confirmed that the Cys114 has a great tendency to form disulfide bonds, since it was associated with β-mercaptoethanol [97].

Considering that TTR is mainly composed by β-sheets, the L12P mutation seems to have the biggest impact on the monomer structure. The differences introduced by the A25T

and especially, V30G mutation, appear to be smaller, but in any case, can alter the protein. In TTR Y114C, the mutation and, therefore, the effect on the protein, does not seem to be so significant. In summary, the L12P mutation has the highest impact on TTR structure, followed by A25T, V30G and, at last, Y114C.

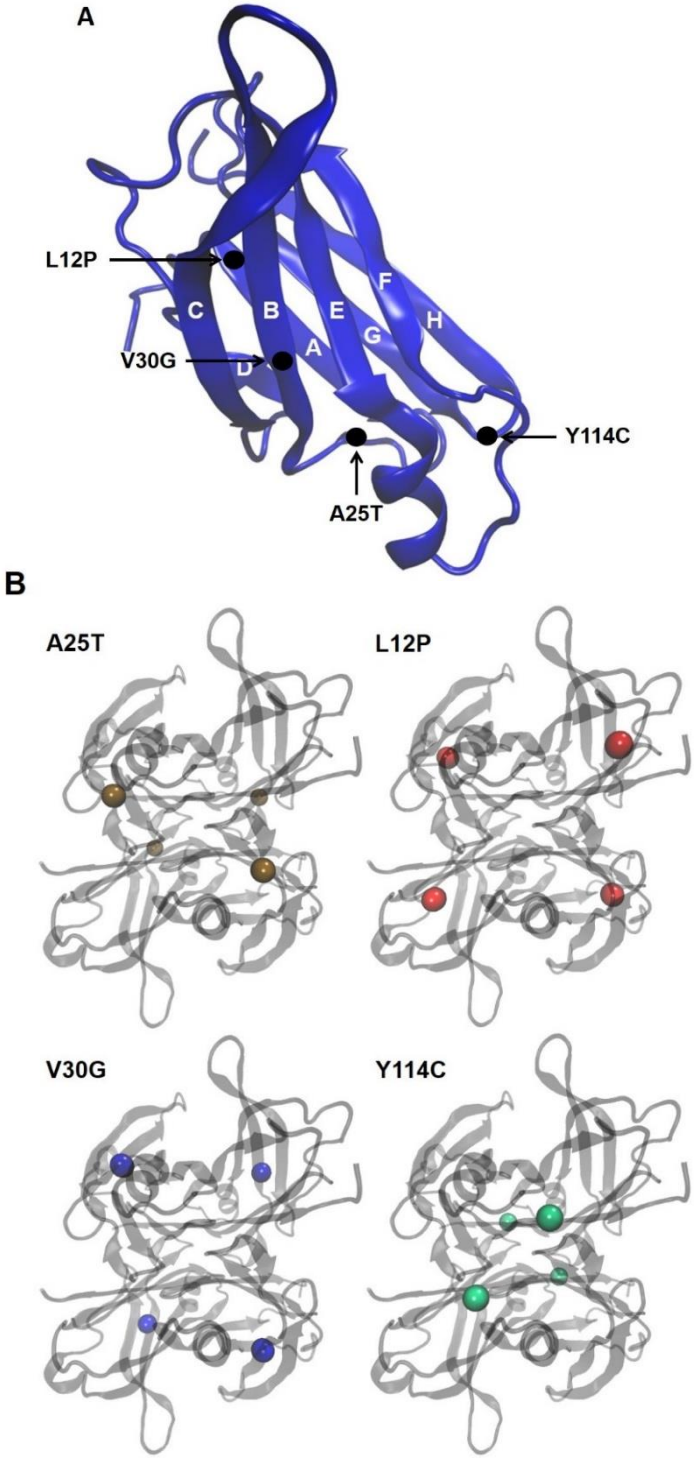

Figure 10. Location of the amino acid substitutions in the monomer (A) and in the tetramer (B) of the TTR variants A25T, L12P, V30G and Y114C.

4.1 *In vitro* kinetics of transthyretin tetramer dissociation

As explained in the introduction, protein stability is crucial for the amyloidogenicity of TTR mutants. For this reason and in the context of the previous paragraphs, we tested the influence of the A25T, L12P, V30G and Y114C mutations on TTR stability, *in vitro*. Tetramer dissociation is required for TTR denaturation by urea [46,98]. Once the tetramer is dissociated, the fast tertiary structural changes can be monitored by Trp fluorescence. Using urea concentrations in the posttransition region for the tertiary structural changes allows to measure tetramer dissociation, as the monomers unfold in a few milliseconds and remain unfolded [57,99]. Considering this, we used 8 M urea and followed unfolding by Trp fluorescence along time (Fig.11 and Table 3).

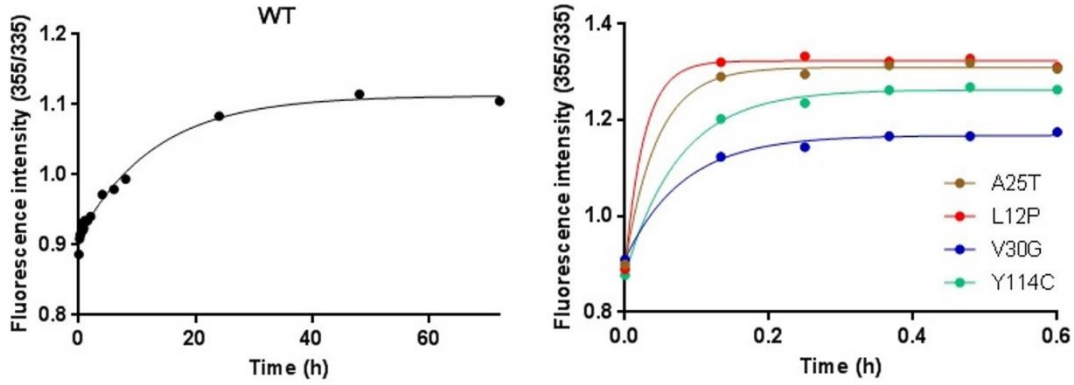

Figure 11. **Leptomeningeal-associated TTR variants kinetic stability in urea.** Graphical representation of the ratio between fluorescence emission intensity at 355 and 335 nm as a function of time. The solid lines through the data are fitted to a single-order exponential function.

Table 3. Dissociation rates of TTR mutants A25T, L12P, V30G and Y114C. Dissociation half-life ($t_{1/2}$) calculated from the fitted data.

	WT	A25T	L12P	V30G	Y114C
$t_{1/2}$	~ 9 hours	~1,9 minutes	~ 1,1 minutes	~ 3,4 minutes	~ 3,1 minutes

We verified that the dissociation half-life ($t_{1/2}$) is much higher for the WT protein as compared to the other variants studied (150-500 times higher). While the $t_{1/2}$ of TTR WT is approximately 9 hours (in 8 M urea, 25ºC), the leptomeningeal-associated variants dissociate in a few minutes (1-3 minutes) under identical conditions. This data suggests that the variant tetramers are extremely destabilized in comparison with the WT protein. With the exception of TTR A25T, there is no report on the dissociation kinetics of these proteins. The $t_{1/2}$ for TTR A25T extrapolated to 0 M urea was calculated to be 2.1 minutes, which is 126-fold faster than that of TTR L55P, a very aggressive mutation [57]. Since the

time-frames for denaturation are so dissimilar, we plotted the variants apart from the WT protein, in an attempt to address the variation in stability between them. The obtained results reveal that the TTR variants L12P and A25T are more unstable than the TTR variants Y114C and V30G. Remarkably, this is in agreement with the yields we obtained when purifying the proteins, with the more stable proteins being recovered at higher levels than the other ones.

4.2 Urea-induced unfolding of transthyretin

After tetramer dissociation, monomer partial unfolding is required for TTR aggregation. Consequently, monomer stability is an important factor to consider when characterizing the changes induced by the mutations. To address this, we incubated the proteins with increasing concentrations of urea for 96 hours, allowing to reach the equilibrium[57,100], and monitored Trp fluorescence, which we used to calculate the fraction unfolded (Fig. 12).

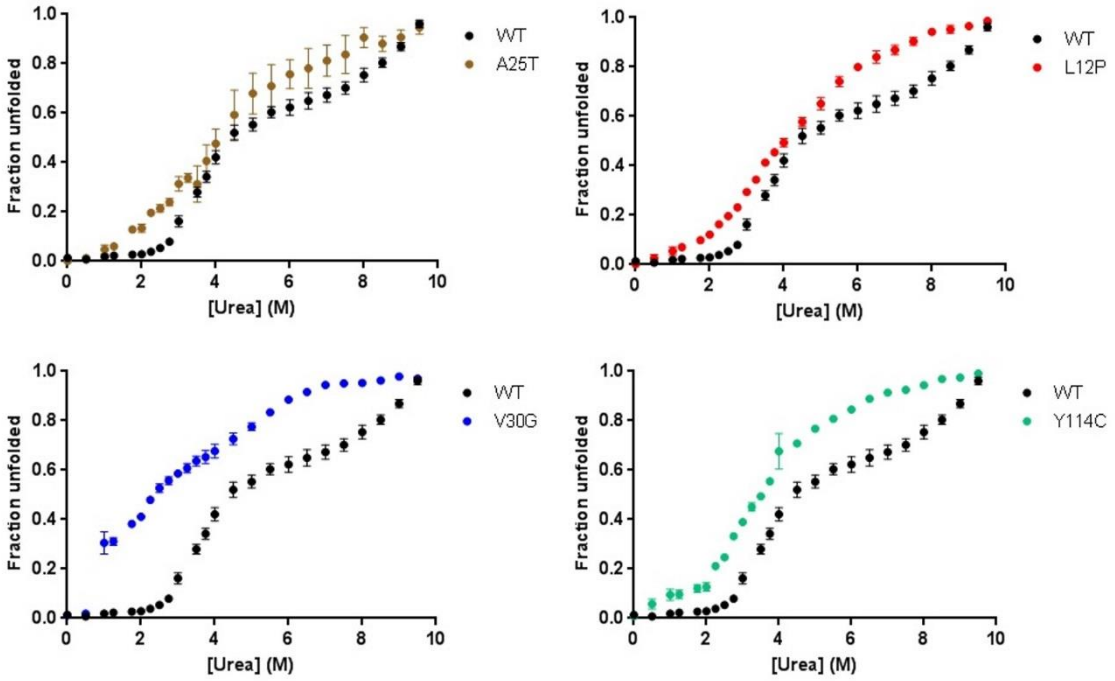

Figure 12. Urea denaturation of leptomeningeal-associated TTR variants. Increase in fraction unfolded as a function of urea concentration. The values represent mean ± s.e.m (n=2).

The first thing that comes to our sight is that the shape of the curves is completely different. For the WT protein, it is described that the stability of the tetramer is related with the stability of the monomer and, so, it is difficult to evaluate the tertiary structure stability with the concentration of TTR normally used in these experiments [58]. It is

possible that the initial phase of the curve we noted for TTR WT, which resembles a lag phase, corresponds to tetramer dissociation. On the contrary, for TTR A25T, the tetramer is so unstable that it dissociates at lower urea concentrations and it seems that the two equilibria are unlinked at 1.44 μM concentration, which is close to the one we have used [58]. In agreement, the lag phase we observed for the WT protein is absent in the curve of TTR A25T, suggesting that it reflects monomer unfolding. The same is true for TTR L12P, which seems even more destabilized than TTR A25T. For TTR Y114C the lag phase is clear, which points to an equilibrium linkage between tetramer dissociation and monomer unfolding. A very short lag phase, which is hidden by the sudden increase in the unfolded fraction, is also seen for TTR V30G. This variant appears to have a slightly higher impact in the quaternary structure stability than TTR Y114C, although less than the TTR mutants A25T and L12P, but a huge impact in tertiary structure stability.

The results obtained thus far suggest that the TTR mutations A25T and L12P affect considerably the quaternary structure, while the V30G mainly destabilizes the tertiary structure. From the four variants, TTR Y114C seems to have the highest quaternary and tertiary structure stability. What is obvious is that these variants start to unfold at very low urea concentrations, even lower than the very destabilized TTR variant L55P [57,58].

4.3 Transthyretin aggregation *in vitro* as a function of pH

To trigger TTR aggregation, not only the tetramer has to dissociate into monomers, but these monomers have to be partially denatured. *In vitro*, the most adopted strategy is to lower the pH [38,46]. According to this, as another step to characterize the proteins of study, we evaluated the pH dependence of their aggregation and compared with the WT form (Fig. 13).

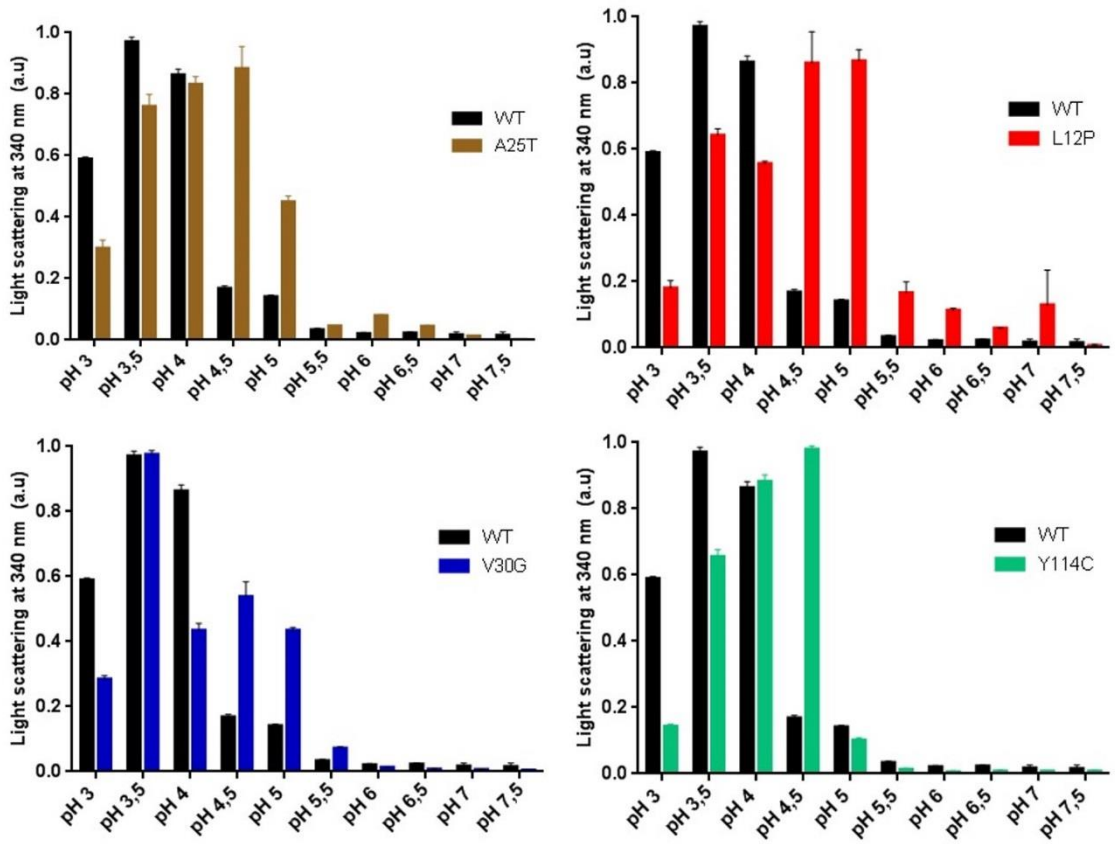

Figure 13. Aggregation of TTR mutants A25T, L12P, V30G and Y114C as a function of pH. The values represent the mean of the raw values of light scattering at 340 nm ± s.e.m (n=3).

We observed that TTR A25T aggregates until pH 6.5, with maximum at 4.5, TTR L12P until pH 7.0, with maximum approximately at 5.0, TTR V30G until pH 5.5, with maximum at 3.5 and, finally, TTR Y114C until pH 5.0, with maximum at 4.5. The WT protein is amyloidogenic until a pH of 5-5.5, with maximum at 3.5.The observations for TTR WT and TTR A25T are consistent with the ones described in the literature [38,62]. For pH lower than 4.0, TTR WT aggregates more than the TTR variants A25T, L12P and Y114C. It is possible that at those low pH, these variants have lost a bigger percentage of their native-like tertiary structure, which is important for TTR aggregation [39]. It is curious that TTR V30G displays the same maximum than TTR WT, suggesting that TTR V30G is more resistant to the changes induced by pH than the other variants. However, TTR V30G still has a considerable aggregation at pH 5 and 5.5, in which the WT protein does not aggregate. Despite these details, it is possible to have a general idea of the stability of these mutants. Since protein stability is related to TTR aggregation, the lower the pH to induce aggregation, the more stable the protein should be. The four variants studied here display a broader aggregation profile than TTR WT, which is shifted to higher aggregation pH. This is especially true for TTR A25T and TTR L12P, which points to a lower overall stability of these mutants, in comparison to the TTR mutants V30G and

Y114C. The profiles exhibited by TTR A25T and TTR L12P are similar to the one of the very unstable leptomeningeal-associated TTR variant D18G [63].

4.4 Tolcapone inhibition of transthyretin aggregation

After this characterization of the TTR variants used in this study, which allowed us to have a general idea of their properties, we proceed to evaluate the potential of tolcapone for treating familial leptomeningeal amyloidosis.

First, we determined the effect of tolcapone on the aggregation of the TTR variants A25T, L12P, V30G and Y114C (Fig. 14).

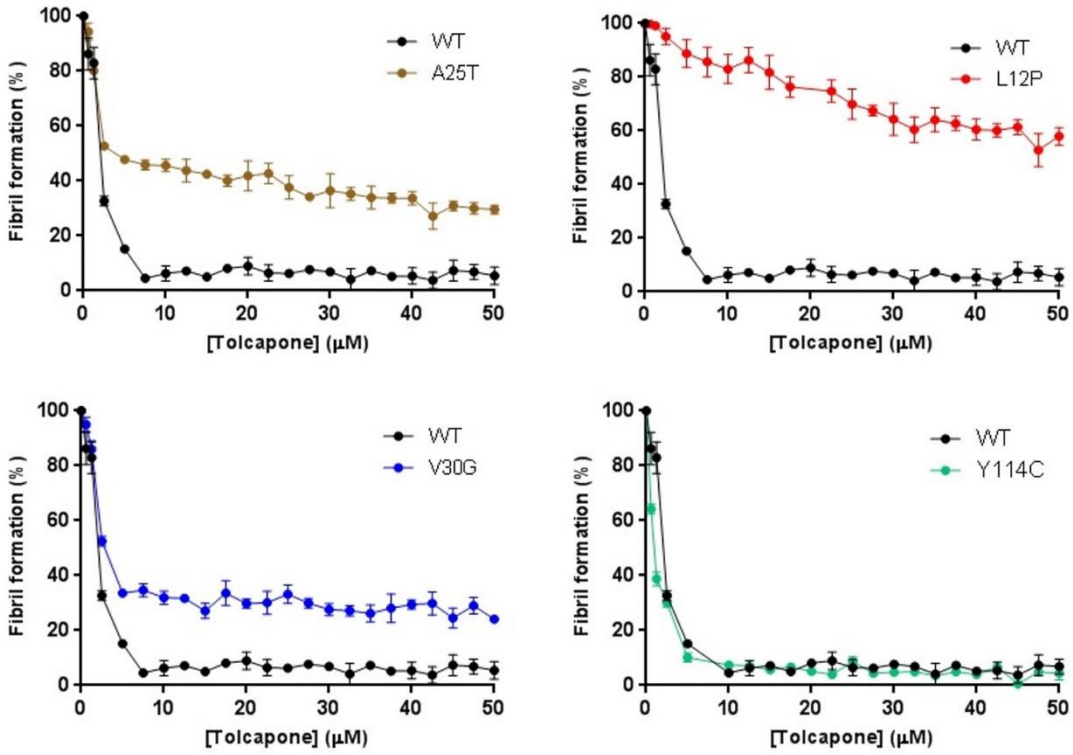

Figure 14. Tolcapone effect over the aggregation of the leptomeningeal-associated TTR variants. Percentage of TTR aggregation as a function of tolcapone concentration. The values are normalized to the maximum, which corresponds to the aggregation in the absence of tolcapone. TTR WT is shown as an example of 100% inhibition. The values represent mean ± s.e.m (n=3).

We verified that tolcapone inhibits up to 71% the aggregation of TTR A25T, 43% of TTR L12P, 76% of TTR V30G and up to 95% of TTR Y114C. The effect on TTR Y114C aggregation is outstanding, being very close to the 100% inhibition displayed by the WT protein in the presence of tolcapone. Remarkably, with 5 μM of tolcapone, that corresponds to less than 2-fold the protein concentration, the inhibition was already evident for the TTR mutants A25T, V30G and Y114C. Ten molar equivalents of

tolcapone (35 μM) reduced around 70% of TTR A25T aggregation, which is similar to the anti-aggregational activity of T_4 at the same pH [62].

4.5 Tolcapone stabilization of transthyretin

After probing that tolcapone can inhibit to more or less extent the aggregation of these extremely destabilized proteins, we wanted to address whether this was due to protein stabilization. For that purpose, we monitored denaturation as a function of urea concentration, as before, but in the presence of 20 or 50 μM tolcapone (Fig. 15). It is important to note that tolcapone does not interfere with Trp fluorescence [44].

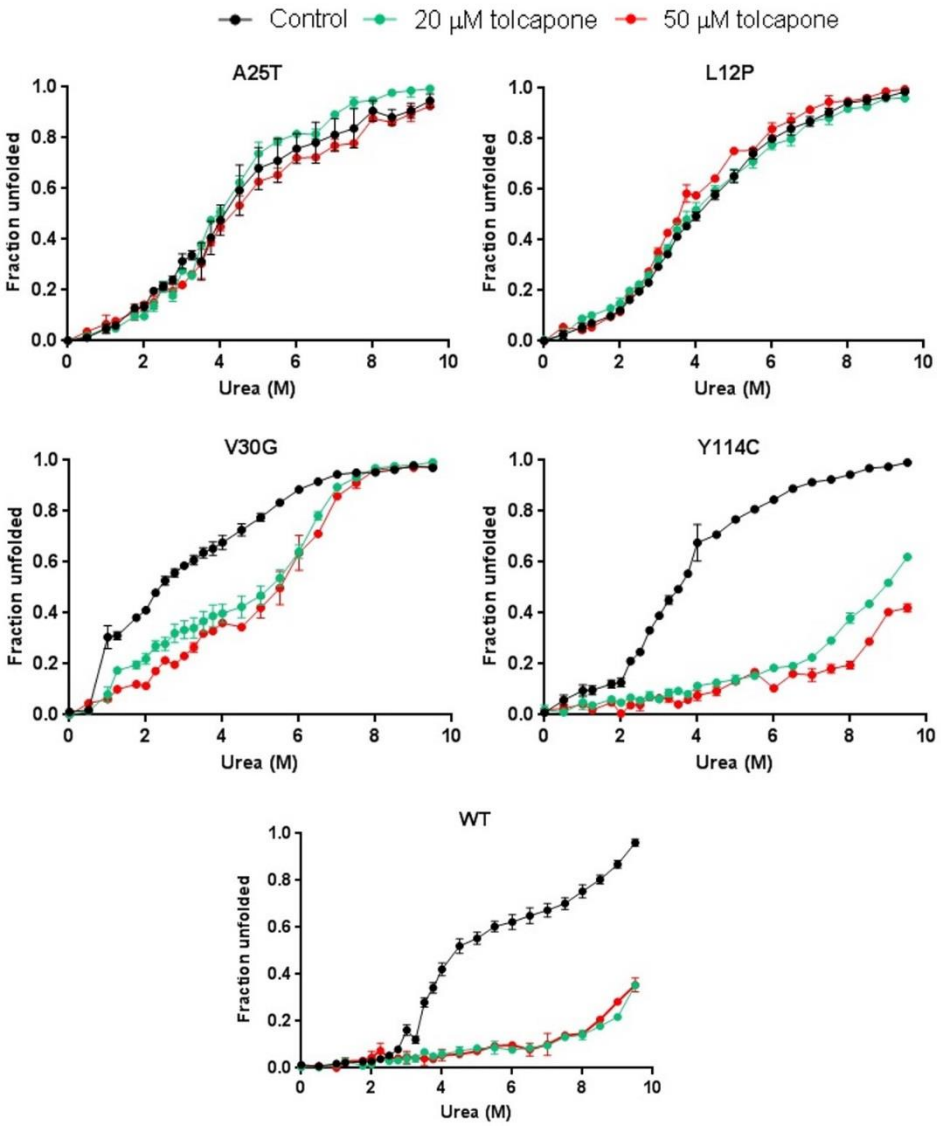

Figure 15. **Urea denaturation of TTR mutants A25T, L12P, V30G and Y114C in the presence of tolcapone.** Increase in fraction unfolded as a function of urea concentration. The curves for TTR WT are shown to compare. Before denaturation the proteins were incubated for 30 minutes with or without tolcapone. The controls were prepared in the same way, without tolcapone. Values represent mean ± s.e.m (n=2).

We observed that the curves are almost overlapping for TTR A25T and TTR L12P, suggesting that tolcapone does not stabilize, at least significantly, these proteins. On the contrary, the stabilizing effect of tolcapone over the TTR variants V30G and Y114C is clear. In these cases, tolcapone displaces the urea curves to the right, meaning that a higher concentration of urea is needed to unfold the protein. The difference is particularly impressive for TTR Y144C. Incubation of this variant with 50 μM tolcapone allows that approximately 60% of the protein is maintained in the native state in 9.5 M urea. This stabilization is similar to the one experienced by the WT protein, with around 70% of the protein remaining in the native state in these conditions. Monitoring the change in stability against urea has been one of the methods adopted for evaluating different approaches to inhibit TTR amyloidogenesis. The curves obtained in the presence of tolcapone resemble the ones described for strategies that are known to impose kinetic stability on TTR by influencing the AB/CD dimer-dimer interface [57,101,102]. In general, there are two ways of increasing the kinetic barrier for tetramer dissociation, one is to decrease the stability of the dissociative state and the other is to increase the stability of the initial tetrameric state. The role of the TTR variant T119M as a *trans*-suppressor of amyloidosis is mediated through the first mechanism, while the effect of small-molecules on TTR aggregation is mediated through the second one [42,60]. In conclusion, tolcapone appears to kinetically stabilize TTR V30G and TTR Y114C, as well as TTR WT, probably due to an increase in tetramer stability.

Another detail we noticed when analyzing the curves is that tolcapone, not only shifts the curve to higher values of urea concentration, but also alters its shape. Interestingly, the curve adopts a format that is similar for the TTR mutants V30G and Y114C and the WT protein. This points to a change in the denaturation pathway of these leptomeningeal-associated mutants, which is closer to the one displayed by TTR WT. Possibly, tolcapone is stabilizing the quaternary structure of these proteins, altering their behavior.

4.6 Resveratrol binding

The fact that there was no distinction in the shape of the urea curves in the presence of tolcapone for TTR A25T and TTR L12P led us to think that, maybe, the native structure of these proteins is so destabilized that the amount of protein present as a tetramer is remarkably lower. In an attempt to address this issue, we used resveratrol (Fig.16). Resveratrol is a small molecule that displays a large increase in its fluorescence quantum yield when bound to at least one of the two thyroid-binding sites in the tetramer. This

molecule does not bind to the TTR monomer (X. Jiang and J. W. Kelly, unpublished results).

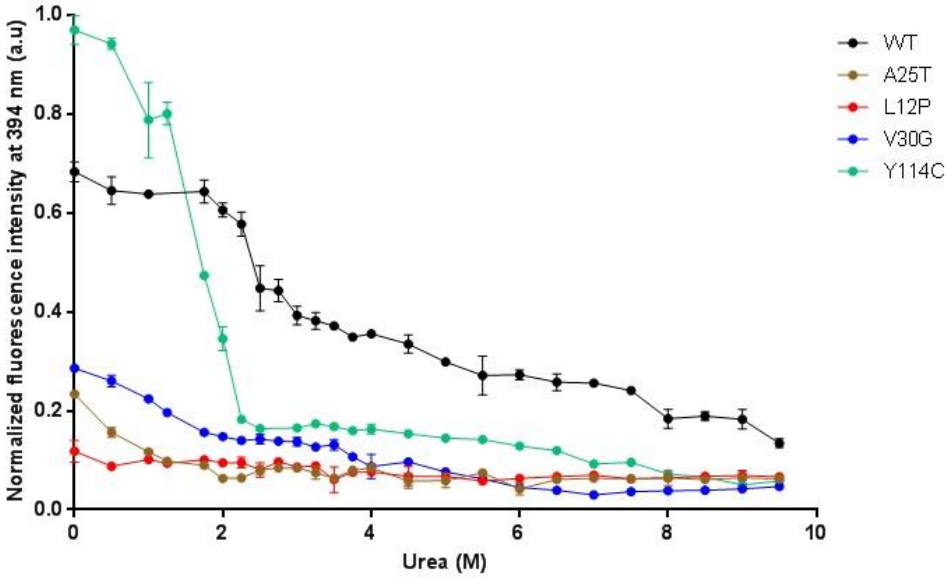

Figure 16. TTR tetramer dissociation curve measured by resveratrol binding of leptomeningeal-associated TTR variants. Normalized fluorescence intensity at 394 nm as a function of urea concentration.

Resveratrol binding has been used to evaluate the quaternary structure of TTR as a function of urea concentration. While Trp fluorescence data accounts for the folded monomer-unfolded monomer equilibrium, resveratrol binding data concerns to the tetramer-folded monomer equilibrium [57,58,62]. When the two curves are nearly coincident, it indicates that the two equilibria are linked [58].

In agreement with the literature[58,62], we observed that the resveratrol binding curve for TTR WT resembles the one obtained by Trp fluorescence, reflecting this thermodynamic linkage. On the contrary, for the TTR variants A25T, L12P and V30G the curves are completely different. TTR A25T and, principally, TTR L12P, do not seem to bind to resveratrol with the same efficiency already at 0 M urea. This suggests that the amount of TTR A25T and TTR L12P adopting a tetrameric structure is very low, or even null, and that what we are monitoring from the beginning by Trp fluorescence is monomer unfolding. The concentration of protein was checked to assure that the difference between variants was not due to different concentrations (data not shown). The fact that the quaternary and tertiary structural stabilities of TTR A25T are not linked at low concentrations was also report by Sekijima *et al*. (2003) [62]. Concerning TTR V30G, the initial binding to resveratrol is not so high as we expected, but it is still slightly higher than the one of TTR A25T and TTR L12P, pointing to a higher ability to maintain or associate into a quaternary structure. Nevertheless, the tetramer is completely lost at low values of urea concentration, which correlates to what we observed in the urea-induced

unfolding curve and indicates that the monomer is the main specie in this curve. From the four variants, the TTR Y114C is the one that resembles more the WT protein. The curve has a marked decrease until 2 M urea and at that point it is supposed that the quaternary structure is lost. It is possible that the equilibria tetramer-folded monomer, folded monomer – unfolded monomer are also linked for TTR Y114C and that the increase in Trp fluorescence at 2 M urea corresponds to the point when the tetramer has converted into monomers and these monomers start to unfold.

Although this is a just a preliminary result, which we intent to repeat, it supports our theory that the TTR variants A25T and L12P have a higher impact in the stability of the protein than TTR V30G and TTR Y114C, affecting its capacity to form a tetramer.

4.7 Tolcapone affinity for A25T, L12P, V30G and Y114C transthyretin variants

In light of these results, our next step was to confirm the binding of tolcapone to these variants. In order to do this, we used ITC, which is the most popular technique for determining the forces that drive the interaction of biological macromolecules (proteins, ligands, hormones and so on). ITC measures the binding equilibrium by direct quantification of the heat exchange during complex formation at a constant temperature [103]. Briefly, there are two identical cells, a sample cell, which contains the protein, in our case, and a reference cell, which contains only buffer. These cells are maintained at the same temperature along the experiment by heaters. When the experiment starts, the ligand, in our case tolcapone, is repeatedly injected into the sample cell in precisely known aliquots. If there is binding, two things can occur, whether the reaction is exothermic and heat is released, or is endothermic and heat is absorbed. In any case, there will be an imbalance of temperature between the two cells and it requires a change in the power applied to the cells. The raw data is the input power required to keep the two cells at the same temperature as a function of time and consists of a series of peaks that return to baseline. Then, this data is transformed into a binding isotherm, which represents the heat of reaction per injection as a function of the ratio of the total ligand concentration to protein concentration. Finally, the isotherm is fitted to an appropriate model and the association constant (K_a), binding enthalpy (ΔH) and the stoichiometry (n) are calculated. The binding free energy (ΔG) and the binding entropy (ΔS) can be obtained from these values, using known equations that relate these thermodynamic parameters [104,105].

The binding of tolcapone to the TTR mutants A25T, L12P, V30G and Y114C is an exothermic reaction, meaning that there is a temperature increase in the sample cell and a simultaneous decrease in the power applied to it (negative peaks) (Fig. 17). As the concentration of tolcapone in the sample cell increases, the signal decreases, since the protein becomes gradually saturated [105]. After conversion of the primary ITC data, the binding parameters were determined from fitting the binding isotherm to an adequate model (Fig.17). Data analysis was done considering two models: (1) two identical and independent binding sites; (2) two identical and cooperative binding sites [91,92]. For TTR A25T and TTR L12P the best fitting was achieved with the second model, while for TTR V30G and TTR Y114C was with the first model. In particular, tolcapone binds to the TTR variants A25T and L12P with negative cooperativity, meaning that, when the first binding site is occupied, there is a loss of affinity for the second binding site [11]. The natural ligand, T_4, as well as most of the small molecules that bind with high affinity to TTR, also bind with negative cooperativity [10,14,43,45,79]. Tolcapone itself binds to TTR WT with negative cooperativity [44]. The appropriate fitting of each curve allowed to obtain the binding parameters (Table 4).

Table 4. **Parameters that describe the binding between tolcapone and TTR mutants A25T, L12P, V30G and Y114C**. Kd: dissociation constant, which is the inverse of the association constant; ΔH – binding enthalpy; ΔG – binding free energy; ΔS – binding entropy; n – Hill coefficient. Values of *n* lower or higher than 1 refer to negatively or positively cooperative binding, respectively, while values of *n* equal to 1 indicate that there is no cooperativity. The numbers 1 and 2 mean that the parameter is associated with the first or second biding site, respectively. Errors: ΔG 0.1 kcal.mol^{-1}, ΔH and -TΔS 0.4 kcal.mol^{-1}.

	A25T	**L12P**	**V30G**	**Y114C**	**WT**
Kd_1 (μM)	0.063	0.036	0.11	0.045	0.021
ΔG_1 (kcal.mol^{-1})	-9.8	-10.2	-9.5	-10.0	-10.5
ΔH_1 (kcal.mol^{-1})	-17.1	-15.0	-12.3	-14.4	-8.7
$-T\Delta S_1$ (kcal.mol^{-1})	7.3	4.8	2.8	4.4	1.8
Kd_2 (μM)	3.1	0.189	0.11	0.045	0.058
ΔG_2 (kcal.mol^{-1})	-7.5	-9.2	-9.5	-10.0	-9.9
ΔH_2 (kcal.mol^{-1})	-12.3	-17.2	-12.3	-14.4	-9.7
$-T\Delta S_2$ (kcal.mol^{-1})	4.8	8.0	2.8	4.4	-0.2
n	0.02	0.61	1	1	0.75

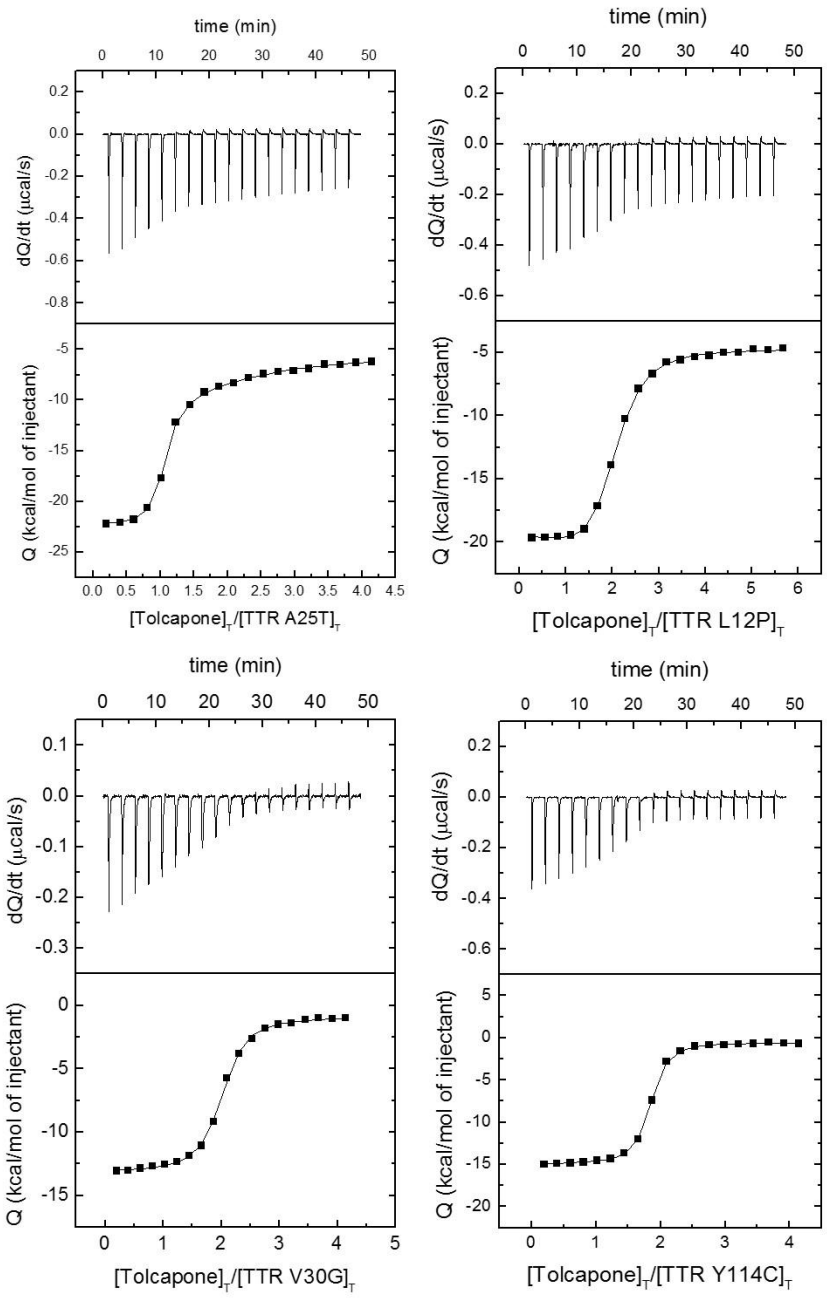

Figure 17. Interaction of leptomeningeal-associated TTR variants with tolcapone assessed by ITC. For each variant, the top panel is the thermogram (thermal power versus time) and the bottom panel is the binding isotherm (normalized heat versus molar ratio of reactants).

Tolcapone binds with high affinity to the four variants, presenting dissociation constants between the low and high nanomolar range. The affinity of tolcapone for the first binding site of the TTR mutants A25T, L12P and Y114C is in the range of TTR WT (Kd_1 = 0.021 µM) and TTR V122I (Kd_1 = 0.056 µM) [44]. However, the loss of affinity for the second binding site of TTR A25T is tremendous, with a value in the micromolar range (Kd_2 = 3.1 µM), which is much higher than the value for TTR WT (Kd_2 = 0.058 µM) and TTR V122I

(Kd_2 = 0.056 μM) [44]. The negative cooperativity for TTR L12P is not so pronounced, maintaining an affinity in the nanomolar range (Kd_2 = 0.189 μM). Since the binding of tolcapone to TTR Y114C is not cooperative, it displays the same high binding affinity for both the first and second binding sites. From the four variants, TTR V30G is the one that binds with lower affinity to tolcapone, but, still, in the nanomolar range. Moreover, in resemblance to TTR Y114C, tolcapone binds to both sites with the same affinity. The absence of cooperativity for the binding of tolcapone was also observed for TTR V122I [44] and for other inhibitors that bind TTR [42,106]. It has been demonstrated by different methods that occupying only one binding site is sufficient to prevent tetramer dissociation. For example, covalent tethering of an inhibitor in a single monomer of TTR tetramer protects the tetramer from dissociation in urea and aggregation under acidic conditions [107]. Additionally, covalent linkage of the A and C subunits of TTR creates a tetramer very resistant to dissociation, both in physiological and denaturing conditions [102]. Despite these evidences, it has been observed that ligands that bind TTR with high affinity and no cooperativity were more efficient at inhibiting dissociation in urea than ligands with strong negative cooperative binding. The reason behind this is that binding to the first and second binding site additively increases the energetic barrier for tetramer dissociation [42]. Accordingly, bivalent inhibitors, which simultaneously occupy both binding sites, were reported as the most powerful TTR stabilizers and aggregation inhibitors [108,109]. Remarkably, these inhibitors are able to tetramerize the extremely unstable leptomeningeal-associated TTR variant D18G, which is largely monomeric, at 25ºC [109]. Taking together all this information, it seems that binding to both sites is important for the activity of kinetic stabilizers. In fact, it was proposed that tolcapone is more efficient than tafamidis at inhibiting the aggregation of TTR WT and the cardiac-related TTR variant V122I because the negative cooperativity is not so evident [44].

The binding of tolcapone to the TTR variants A25T, L12P, V30G and Y114C occurs spontaneously, as ΔG is negative. The value of ΔG depends on ΔH and ΔS, a relation that is translated by the equation $\Delta G = \Delta H - T\Delta S$ [104] (Fig. 18). So, when the value of ΔH and $-T\Delta S$ is negative, there is a favorable contribution for the binding process.

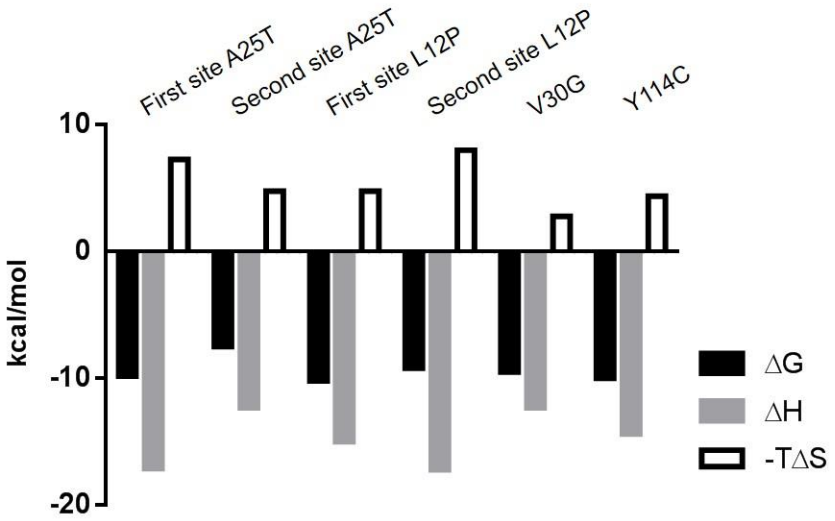

Figure 18. Enthalpic and entropic contributions to the binding of tolcapone to TTR mutants A25T, L12P, V30G and Y114C. Graphical representation of ΔG, ΔH and -TΔS for binding to the first and second binding site. In the case of V30G TTR and Y114C TTR, the binding parameters for both sites are the same.

The change in enthalpy results from the balance between the interactions that are lost upon binding, like the ones established by the protein and ligand with the solvent, and the interactions that are formed. The total entropy change associated with binding depends on, among other factors, the solvent entropy change when it is released from the binding site and the conformational entropy change of the protein and ligand associated with the different freedom in the protein-ligand complex [103,104]. In this case study, the binding is enthalpically favorable, but entropically unfavorable, similarly to the binding of tolcapone to TTR V122I [44]. This suggests the formation of specific noncovalent interactions between the protein and the ligand, like hydrogen bonds or salt bridges, that restrict their movement, leading to an unfavorable entropy change. The negative correlation between enthalpy and entropy is known as enthalpy-entropy compensation and it has been observed for most protein-ligand complexes [110]. This phenomenon hinders drug design, as small changes introduced in the ligand in order to improve the enthalpy or entropy of interaction may not increase the binding affinity[111,112].

4.8 Crystal structures of Transthyretin/tolcapone complexes

To assess the interactions that drive binding of tolcapone to our variants, we obtained the co-crystal structure of tolcapone with TTR A25T, TTR V30G and TTR Y114C, at a resolution of 1.6, 1.2 and 1.9 Å, respectively. We have also crystallized TTR L12P with tolcapone but the crystals formed were too small and did not diffract well. The fact that this variant is more difficult to crystallize is in agreement with the results presented up to

this point, which point to TTR L12P as the most unstable mutant of the four and the less responsive to the effect of tolcapone.

The TTR/tolcapone complexes analyzed in the present work, crystallized in the same space group as the TTR WT/tolcapone complex[44], $P2_12_12$, suggesting that the overall structure is maintained. Actually, there is practically an overlapping between the co-crystal structure of TTR A25T, TTR V30G and TTR Y114C with tolcapone and the co-crystal structure of TTR WT with tolcapone (Fig. 19, A-D). There is one dimer (monomers A and B) in the asymmetric unit, as it happens in most of the TTR crystallographic structures. The crystallographic 2-fold symmetry axis is generally used to create the structure of the tetramer from the structure of the dimer in the asymmetric unit [9,55]. Also in the absence of tolcapone, TTR A25T and TTR Y114C were found to crystalize in the same space group than TTR WT [93,97]. The high-resolution of the crystals allows to unequivocally place tolcapone in the T_4 – binding sites formed by the AB/CD dimer-dimer interface (Fig. 19, E). Indeed, tolcapone was found in two symmetrically equivalent binding modes, related by a 180º rotation. Tolcapone binds to the TTR variants A25T, V30G and Y114C in the forward mode, with the 4-methyl-phenyl ring occupying the inner binding cavity and the 3,4-dihydroxy-5-nitrophenyl ring of tolcapone oriented to the outer biding cavity (Fig. 19, F-I). In this orientation, the 4-methyl-phenyl ring establishes hydrophobic interactions with the residues in the HBPs 2/2' and 3/3' and the 3,4-dihydroxy-5-nitrophenyl ring is surrounded by the residues in the HBPs 2/2' and 1/1'. Additionally, in the outer binding cavity, the hydroxyl groups of the nitrophenyl ring form electrostatic interactions with Lys15 from both chains which, in turn, form salt bridges with Glu54/54'. These contacts were also reported for the binding of tolcapone to TTR WT and the cardiac-related TTR variant V122I [44].

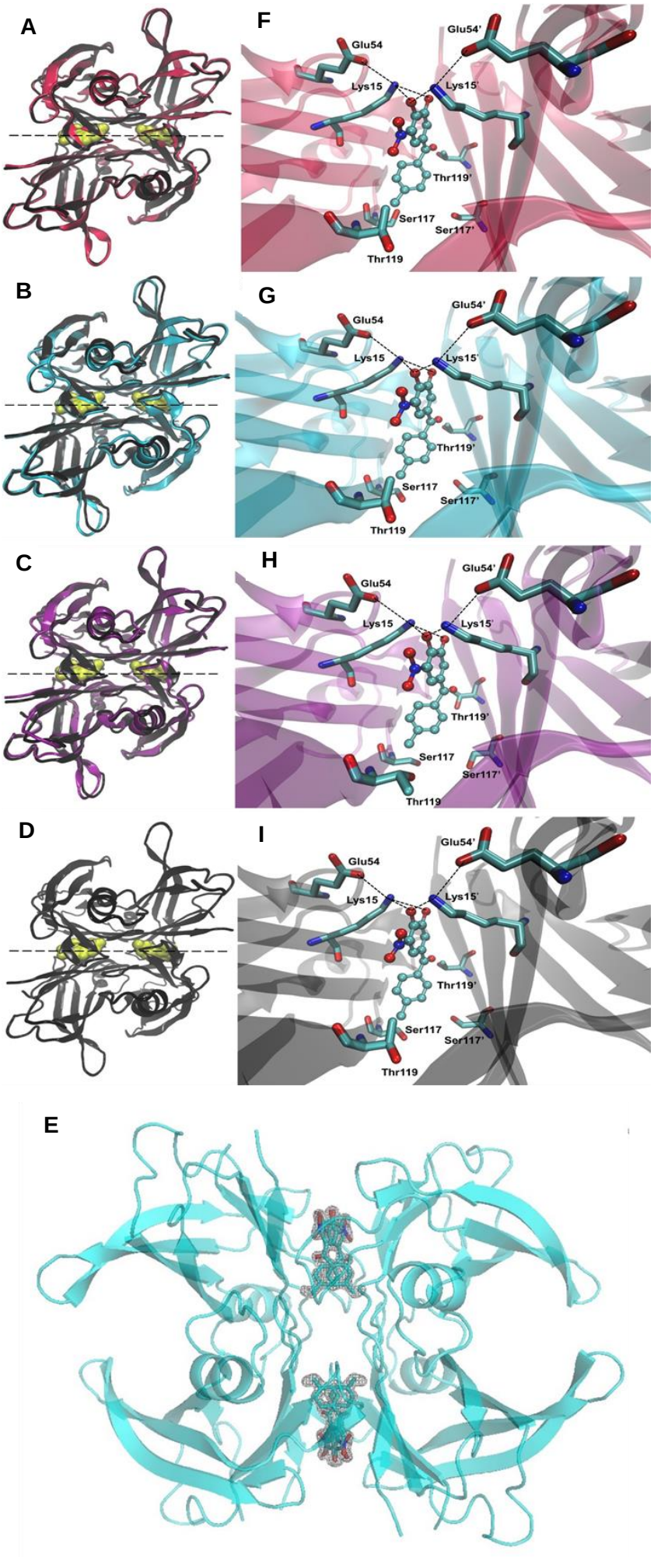
A
F
Glu54
Glu54'
Lys15
Lys15'
Thr119'
Ser117
Ser117'
Thr119
B
G
C
H
D
I
E

Figure 19. Crystal structures of A25T TTR/tolcapone, V30G TTR/tolcapone and Y114C TTR/tolcapone complexes. Cartoon representation of (A) TTR A25T, (B) TTR V30G and (C) TTR Y114C bound to tolcapone (yellow surface). The dashed line evidences the crystallographic axis. The structure of the TTR WT/tolcapone complex (PDB: 4D7B) is shown in black for comparison (D). The electron density map of the two T_4-binding pockets of tolcapone in the TTR V30G/tolcapone complex is depicted as an example (E). Magnified image of tolcapone (CPK representation) bound to one of the TTR A25T (F), TTR V30G (G), TTR Y114C (H) and TTR WT (I) binding sites, formed by the chain A (on the left) and C (on the right). The residues that are known to form important interactions with TTR ligands are depicted. The dashed lines indicate the interactions observed

Together, we verified that the binding of tolcapone to the TTR mutants A25T, V30G and Y114C involves the establishment of specific contacts, which might justify why it is enthalpically driven. Additionally, these interactions are similar to the ones described for TTR WT and TTR V122I [44], explaining why it binds to TTR A25T, TTR V30G and TTR Y114C with high affinity. To sum up, tolcapone binding to these leptomeningeal-associated variants brings the dimers together, through the formation of hydrophobic and polar interactions, contributing to stabilize the native state of TTR [41,113,114].

5. Conclusion

Protein aggregation is associated with several disorders, as the highly incident AD and PD, or type II diabetes [18]. TTR aggregation is linked to a variety of diseases, each of them with a different phenotype. While the WT protein causes SSA, a sporadic, late-onset disease, FAC, FAP and familial leptomeningeal amyloidosis are related to TTR variants and follow an autosomal dominant inheritance pattern [19–25]. Among other disadvantages, the current therapy for these disorders, liver or combined liver and heart transplantation [28,73], is not suitable for familial leptomeningeal amyloidosis, a rare form of TTR amyloidosis that affects the CNS [22–25]. The pursuit of other therapies for TTR amyloidosis and the discovery of a mutation that protects from disease through tetramer stabilization led to the development of hundreds of small molecule inhibitors of protein aggregation. These molecules bind with high affinity to one or both T_4-binding sites and prevent TTR tetramer dissociation and, consequently, aggregation, by kinetically stabilizing the native state [14,41,42,60]. One of these compounds is tolcapone, which was recently discovered by our group using a drug repositioning strategy. Tolcapone is approved by the FDA for PD and we obtained evidences that it stabilizes TTR, both *in vitro* and *in vivo*, and inhibits very efficiently its aggregation, even more than tafamidis, the only small molecule in the market for the treatment of TTR amyloidosis so far. Moreover, we previously observed that tolcapone is able to inhibit the aggregation of the leptomeningeal-associated TTR variant A25T [44]. This, together with the fact that tolcapone can cross the BBB, turn it into the best viable option for treating familial leptomeningeal amyloidosis, which cannot be addressed with any of the strategies available at the time.

To explore this idea, we have carried out this study, in which we described in detail the activity of tolcapone on four TTR mutants linked to familial leptomeningeal amyloidosis, TTR A25T, TTR L12P, TTR V30G and TTR Y114C. These variants, especially TTR L12P and TTR V30G, are poorly described on the literature. Therefore, we started with a slight characterization of the proteins and then we tested the effect of tolcapone on their stability and aggregation and examined its binding.

Protein stability plays an essential role in TTR aggregation, being one major determinant of the amyloidogenicity of TTR mutants [57,58]. Putting the results together, which were obtained by different techniques, like monitoring urea-induced unfolding and resveratrol binding, we can affirm that the selected leptomeningeal-associated variants are extremely destabilized in relation to TTR WT. Considering them from the less to the most stable, we have TTR L12P, TTR A25T, TTR V30G and TTR Y114C. Moreover, it seems

that these variants fall into two groups, one with the TTR variants L12P and A25T and the other with the TTR variants V30G and Y114C. In the first group, the proteins aggregate at higher pH, especially TTR L12P, closer to the physiological pH, making them even more dangerous. On the contrary, TTR V30G and TTR Y114C do not aggregate at pH higher than 5-5.5. Although the quaternary structure of the four mutants is extremely destabilized in comparison to TTR WT, the A25T and L12P mutations appear to have such a high impact in TTR stability that they lower the ability of the protein to adopt the functional native tetrameric structure. Taking into consideration that tolcapone acts by binding tetrameric TTR and stabilizing the dimer-dimer interface, if a part, or the majority of the protein in solution, is not tetrameric, the binding and activity of tolcapone will be dramatically affected. Importantly, this does not imply that tolcapone cannot bind to the TTR variants A25T and L12P. In fact, tolcapone binds with high affinity to these mutants, similarly to TTR V30G and TTR Y114C, and inhibits their aggregation, as long as there is tetrameric protein available. It is possible that in the conditions used for examining the stabilizing effect of tolcapone over the variants, there is few amount of tetrameric TTR A25T and TTR L12P, and therefore, the monitored stabilizing activity of tolcapone is low or even null. On the other hand, the quaternary structure of TTR V30G and TTR Y114C is significantly stabilized by tolcapone. Tolcapone is particularly effective for TTR Y114C, which is the variant that most resembles TTR WT, maintaining a portion of the protein in the native state, even in extreme denaturing conditions, and inhibiting almost completely its aggregation.

In conclusion, we validated that tolcapone can become the first small molecule treatment available for familial leptomeningeal amyloidosis. We confirmed that it binds with high efficiency to TTR mutants related to this disorder, stabilizing them and, consequently, inhibits their aggregation. However, it should be noted that, if the portion of protein present as tetramer is considerably diminished, the activity of tolcapone will be affected. This raises the possibility of adopting a personalized therapy approach, in which the patient is given tolcapone, according to the mutation responsible for its disease. Considering this, we are thinking to find an approach that allows to discriminate whether tolcapone will be efficient or not, based on a preliminary prediction of the stability of the TTR variant.

Furthermore, the results of this study have proven the high efficiency of tolcapone, demonstrated in the first place for the WT protein and the FAC-related mutant V122I, and have expanded the set of variants that can be targeted with this drug. The high affinity and efficiency of tolcapone for the different TTR mutants, the fact that it can cross the BBB and that it is approved by the FDA, constitute powerful reasons to continue exploring its applicability. Namely, tolcapone can be used as a scaffold for the rational

design of more powerful derivatives, destined to improve the therapy for TTR amyloidosis.

6. Future perspectives

Even though one of the strongest theories regarding TTR aggregation defends that it involves acid-mediated denaturation, which could be achieved *in vivo* in the lysosomes, the exact mechanism remains unclear. In fact, it was observed that the WT protein dissociates on a biologically relevant timescale under physiological conditions [115]. Therefore, it is important to test the activity of inhibitors in different environments. We have reasons to believe that tolcapone will perform well for the leptomeningeal-associated variants under native conditions. Tolcapone binds and stabilizes TTR WT and TTR V30M in human plasma and, more importantly, after oral administration in healthy volunteers [44]. In addition, tolcapone inhibits TTR aggregation induced by proteolytic cleavage at physiological pH [116]. In any case, we intend to analyze the effect of tolcapone over leptomeningeal-associated TTR variants in conditions close to physiological. Since it was reported that TTR A25T aggregates in the CSF [93], we plan to investigate whether tolcapone can inhibit the aggregation of our study variants in this milieu.

Several results accumulated on the binding and efficiency of small molecule inhibitors of TTR aggregation, suggest that a strong negative cooperativity reduces their activity [42,44,108,109,116]. For example, the bivalent inhibitor mds84 is one of the most potent TTR stabilizers and inhibitors of TTR aggregation [108,116]. Moreover, tolcapone inhibits more efficiently the aggregation of TTR than tafamidis, whether it is induced by acid denaturation or by proteolytic cleavage. It was proposed that the basis for this, is the lower negative cooperativity of tolcapone on binding to TTR [44,116]. Even though tolcapone displays a higher binding affinity for the second binding site, the dichlorophenyl ring of tafamidis seems to dock better to the first binding site than the methyl-phenyl ring of tolcapone [44]. Accordingly, a study on diflunisal analogues revealed that compounds with two halogens in the hydrophobic ring perform better than compounds lacking halogens or with one halogen [114]. For these reasons, in the near future, we will explore two strategies to improve the activity of tolcapone: a combined therapy with tolcapone and tafamidis, using different tolcapone:tafamidis ratio, and a chimeric compound, which is already synthetized, combining the upper ring of tolcapone and the lower ring of tafamidis.

7. References

1. Kanai, M., Raz, A. & Goodman, D. S. Retinol-binding protein: the transport protein for vitamin A in human plasma. *J. Clin. Invest.* **47,** 2025–44 (1968).
2. Robbins, J. & Rall, J. E. Proteins associated with the thyroid hormones. *Physiol. Rev.* **40,** 415–489 (1960).
3. Schreiber, G. & Richardson, S. J. The Evolution of Gene Expression, Structure and Function of Transthyretin. *Comp. Biochem. Physiol. Part B Biochem. Mol. Biol.* **116,** 137–160 (1997).
4. Haggen, G. & Elliott, W. Transport of thyroid hormones in serum and cerebrospinal fluid. *J Clin Endocrinol Metab* **37,** 415–422 (1973).
5. Harms, P. J. *et al.* Transthyretin (prealbumin) gene expression in choroid plexus is strongly conserved during evolution of vertebrates. *Comp. Biochem. Physiol. -- Part B Biochem.* **99,** 239–249 (1991).
6. Schreiber, G. *et al.* Thyroxine transport from blood to brain via transthyretin synthesis in choroid plexus. *Am. J. Physiol.* **258,** R338-R345 (1990).
7. Jacobsson B., Collins V., Grimelius L., Pettersson T., S. B. and C. A. Transthyretin Immunoreactivity in Human and Porcine Liver, Choroid Plexus, and Pancreatic Islets. *J. Histochem. Cytochem.* **37,** 31-37 (1989).
8. Blake, C. C. F., Geisow, M. J., Swan, I. D. A., Rerat, C. & Rerat, B. Structure of human plasma prealbumin at 2.5 A resolution. A preliminary report on the polypeptide chain conformation, quaternary structure and thyroxine binding. *J. Mol. Biol.* **88,** 1–12 (1974).
9. Blake, C. C. F., Geisow, M. J., Oatley, S. J., Rérat, B. & Rérat, C. Structure of prealbumin: Secondary, tertiary and quaternary interactions determined by Fourier refinement at 1.8 Å. *J. Mol. Biol.* **121,** 339–356 (1978).
10. Fergunson RN, Edelhoch H, Saroff HA, Robbins J, C. H. Negative cooperativity in the binding of thyroxine to human serum prealbumin. Preparation of tritium-labeled 8-anilino-1-naphthalenesulfonic acid. *Biochemistry* **14,** 282–289 (1975).
11. Neumann, P., Cody, V. & Wojtczak, A. Structural basis of negative cooperativity in transthyretin. *Acta Biochim. Pol.* **48,** 867–875 (2001).
12. Blake C. C. F., O. S. J. Protein-DNA and protein-hormone interactions in prealbumin: a model of the thyroid hormone nuclear receptor? *Nat. Publ. Gr.* **268,** 115–120 (1977).
13. Wojtczak, A., Cody, V., Luft, J. R. & Pangborn, W. Structures of human transthyretin complexed with thyroxine at 2.0 A resolution and 3',5'-dinitro-N-acetyl-L-thyronine

at 2.2 A resolution. *Acta Crystallogr. D. Biol. Crystallogr.* **D52,** 758–765 (1996).

14. Johnson, S. M. *et al.* Native state kinetic stabilization as a strategy to ameliorate protein misfolding diseases: A focus on the transthyretin amyloidoses. *Acc. Chem. Res.* **38,** 911–921 (2005).
15. Oatley, S. J., Blaney, J. M., Langridge, R. & Kollman, P. A. Molecular Mechanics Studies of Thyroid Hormone-Protein Interactions: The Interaction of T4 and T3 with Prealbumin. *Biopolymers.* **23,** 2931–2941 (1984).
16. Ciszak, E., Cody, V. & Luft, J. Crystal structure determination at 2.3-A resolution of human transthyretin-3',5'-dibromo-2',4,4',6-tetrahydroxyaurone complex. *Proc. Natl. Acad. Sci. U. S. A.* **89,** 6644–6648 (1992).
17. Westermark, P. *et al.* Amyloid : Toward terminology clarification Report from the Nomenclature Committee of the International Society of Amyloidosis Amyloid : Toward terminology clarification. **12,** 1-4 (2009).
18. Chiti, F. & Dobson, C. M. Protein misfolding, functional amyloid, and hauman disease. *Annu. Rev. Biochem.* **75,** 333–366 (2006).
19. Costa, P. P., Figueira, A. S. & Bravo, F. R. Amyloid fibril protein related to prealbumin in familial amyloidotic polyneuropathy. *Proc. Natl. Acad. Sci. U. S. A.* **75,** 4499–503 (1978).
20. Aniel J Acobson, D. R. *et al.* Variant-sequence transthyretin (isoleucin 122) in late-onset cardiac amyloidosis in black americans. *N. Engl. J. Med.* **336,** 466–473 (1997).
21. Westermark, P., Sletten, K., Johansson, B. & Cornwell, G. G. Fibril in senile systemic amyloidosis is derived from normal transthyretin. *Proc. Natl. Acad. Sci. U. S. A.* **87,** 2843–2845 (1990).
22. Martin, S. E., Benson, M. D. & Hattab, E. M. The pathologic spectrum of oculoleptomeningeal amyloidosis with Val30Gly transthyretin gene mutation in a. *Hum. Pathol.* **45,** 1105–1108 (2014).
23. Mccolgan, P. *et al.* Oculoleptomeningeal Amyloidosis associated with transthyretin Leu12Pro in an African patient. **262,** 228–234 (2015).
24. Ueno, S., Uemichi, T., Yorifuji, S. & Tarui, S. A novel variant of transthyretin (Tyr114 to Cys) deduced from nucleotide sequences of gene fragments from familial amyloidotic polyneuropathy in japanese sibling cases. *Biochem. Biophys. Res. Commun.* **169,** 143–147 (1990).
25. Llull, L., Berenguer, J., Yagüe, J. & Graus, F. Leptomeningeal amyloidosis due to A25T TTR mutation : A case report. *Neurologia*. **29,** 382-384 (2014).
26. Goren, H. & Steinberg, M. C. Familial oculoleptomeningeal amyloidosis. *Brain*. **103,** 473–495 (1980).
27. Cornwell, G. G., Sletten, K., Johansson, B. & Westermark, P. Evidence that the

amyloid fibril protein in senile systemic amyloidosis is derived from normal prealbumin. *Biochem. Biophys. Res. Commun.* **154,** 648–653 (1988).

28. Rapezzi, C. *et al.* Transthyretin-related amyloidoses and the heart: a clinical overview. *Nat. Rev. Cardiol.* **7,** 398–408 (2010).
29. Gorevic, P. D., Prelli, F. C., Wright, J., Pras, M. & Frangione, B. Systemic senile amyloidosis. Identification of a new prealbumin (Transthyretin) variant in cardiac tissue: immunologic and biochemical similarity to one form of Familial Amyloidotic Polyneuropathy. *J.Clin.Invest.* **83,** 836–843 (1989).
30. Andrade, C. A peculiar form of peripheral neuropathy. *Brain* **75,** 408–427 (1952).
31. Araki, S., Mawatari, S. & Ohta, M. Polyneuritic Amyloidosis in a Japanese Family. *Arch Neurol*. **18,** 593–602 (2015).
32. Saraiva, M., Birken, M., Costa,P. & Goodman, D. Amyloid Fibril Protein in Familial Amyloidotic Polyneuropathy, Portuguese Type Definition of Molecular Abnormality in Transthyretin (Prealbumin). **74,** 104–119 (1984).
33. Parman, Y. *et al.* Sixty years of transthyretin familial amyloid polyneuropathy (TTR-FAP) in Europe: where are we now? A European network approach to defining the epidemiology and management patterns for TTR-FAP. *Curr. Opin. Neurol.* **29 Suppl 1,** S3–S13 (2016).
34. Nakamura, M. *et al.* Neuroradiologic and clinicopathologic features of oculoleptomeningeal type amyloidosis. *Neurology.* **65,** 1051–1056 (2005).
35. Hagiwara, K. *et al.* Highly selective leptomeningeal amyloidosis with transthyretin variant ala25thr. *Neurology*. **72,** 1358–1359 (2009).
36. Brett, M. *et al.* Transthyretin Leu12Pro is associated with systemic , neuropathic and leptomeningeal amyloidosis. *Brain*. **122,** 183–190 (1999).
37. Petersen, R. B., Goren, H., Cohen, M., Richardson, S. L. & Tresser, N. Transthyretin Amyloidosis : A New Mutation - Associated with Dementia. *Annals of Neurology*. **41,** 307–313 (1997).
38. Colon, W. & Kelly, J. W. Partial Denaturation of Transthyretin Is Sufficient for Amyloid Fibril Formation in Vitro. *Biochemistry.* **31,** 8654–8660 (1992).
39. Zhihong, L., Wilfredo C. and & Kelly, J. W. The Acid-Mediated Denaturation Pathway of Transthyretin Yields a Conformational Intermediate That Can Self-Assemble into Amyloid. *Biochemistry*. **35,** 6470–6482 (1996).
40. Foss, T. R., Wiseman, R. L. & Kelly, J. W. The pathway by which the tetrameric protein transthyretin dissociates. *Biochemistry.* **44,** 15525–15533 (2005).
41. Connelly, S., Choi, S., Johnson, S. M., Kelly, J. W. & Ian, A. Structure-based design of kinetic stabilizers that ameliorate the transthyretin amyloidoses. *Curr. Opin. Struct. Biol.* **20,** 54–62 (2011).

42. Hammarstrom, P. Prevention of Transthyretin Amyloid Disease by Changing Protein Misfolding Energetics. *Science.* **299,** 713–716 (2003).
43. Bulawa, C. E. *et al.* Tafamidis , a potent and selective transthyretin kinetic stabilizer that inhibits the amyloid cascade. *PNAS*. **109**, 3–8 (2012).
44. Sant'Anna, R. *et al.* Repositioning tolcapone as a potent inhibitor of transthyretin amyloidogenesis and associated cellular toxicity. *Nat. Commun.* **7,** 10787 (2016).
45. Tojo, K., Sekijima, Y., Kelly, J. W. & Ikeda, S. ichi. Diflunisal stabilizes familial amyloid polyneuropathy-associated transthyretin variant tetramers in serum against dissociation required for amyloidogenesis. *Neurosci. Res.* **56,** 441–449 (2006).
46. Jiang, X. *et al.* An Engineered Transthyretin Monomer that Is Nonamyloidogenic, Unless It Is Partially Denatured†. *Biochemistry.* **40,** 11442–11452 (2001).
47. Shirahama, T. & Cohen, A. S. Intralysosomal formation of amyloid fibrils. *Am. J. Pathol.* **81,** 101–116 (1975).
48. Hurshman, A. R., White, J. T., Powers, E. T. & Kelly, J. W. Transthyretin Aggregation under Partially Denaturing Conditions Is a Downhill Polymerization. *Biochemistry.* **43,** 7365–7381 (2004).
49. Knowles, T. P. J., Vendruscolo, M. & Dobson, C. M. The amyloid state and its association with protein misfolding diseases. *Nat. Rev. Mol. Cell Biol.* **15,** 384–96 (2014).
50. Rochet, J. C. & Lansbury, P. T. Amyloid fibrillogenesis: Themes and variations. *Curr. Opin. Struct. Biol.* **10,** 60–68 (2000).
51. Faria, T. *et al.* A look into amyloid formation by transthyretin: aggregation pathway and a novel kinetic model. *Phys. Chem. Chem. Phys.* **17,** 7255–7263 (2015).
52. Khurana, R. *et al.* Mechanism of thioflavin T binding to amyloid fibrils. *J. Struct. Biol.* **151,** 229–238 (2005).
53. Marcoux, J. *et al.* A novel mechano-enzymatic cleavage mechanism underlies transthyretin amyloidogenesis. *EMBO Mol. Med.* **7,** 1337–1349 (2015).
54. Ihse, E. *et al.* Amyloid fibrils containing fragmented ATTR may be the standard fibril composition in ATTR amyloidosis. *Amyloid.* **20,** 142–150 (2013).
55. Hörnberg, A., Eneqvist, T., Olofsson, A., Lundgren, E. & Sauer-Eriksson, a E. A comparative analysis of 23 structures of the amyloidogenic protein transthyretin. *J. Mol. Biol.* **302,** 649–669 (2000).
56. Sebastião, M. P., Saraiva, M. J. & Damas, A. M. The crystal structure of amyloidogenic Leu55Pro transthyretin variant reveals a possible pathway for transthyretin polymerization into amyloid fibrils. *J. Biol. Chem.* **273,** 24715–24722 (1998).
57. Hammarström, P., Jiang, X., Hurshman, A. R., Powers, E. T. & Kelly, J. W.

Sequence-dependent denaturation energetics: a major determinant in amyloid disease diversity. *Proc. Natl. Acad. Sci. U. S. A.* **99,** 16427–16432 (2002).

58. Babbes, A., Powers, E. T. & Kelly, J. W. Quantification of the thermodynamocally linked quaternary and tertiary structural stabilities of transthyretin and its disease-associated variants - the relationship between stability and amyloidosis. *Biochemistry*. **47,** 6969–6984 (2008).
59. Lashuel, H. A., Wurth, C., Woo, L. & Kelly, J. W. The Most Pathogenic Transthyretin Variant , L55P, Forms Amyloid Fibrils under Acidic Conditions and Protofilaments under Physiological Conditions. *Biochemistry*. **38**, 13560–13573 (1999).
60. Hammarstrom, P. Trans-Suppression of Misfolding in an Amyloid Disease. *Science.* **293,** 2459–2462 (2001).
61. Sekijima, Y. *et al.* The biological and chemical basis for tissue-selective amyloid disease. *Cell*. **121,** 73–85 (2005).
62. Sekijima, Y., Hammarström, P., Matsumura, M. & Shimizu, Y. Energetic Characteristics of the New Transthyretin Variant A25T May Explain Its Atypical Central Nervous. *Lab. Investig.* **83,** 409–417 (2003).
63. Hammarström, P. *et al.* D18G Transthyretin is Monomeric, Aggregation Prone, and Non-Detectable in Plasma and Cerbrospinal Fluid - A Prescription for CNS Amyloidosis? *Biochemistry.* **42,** 6656–6663 (2003).
64. Goldberg, M. S. & Jr, P. T. L. Is there a cause-and-effect relationship between α - synuclein fibrillization and Parkinson ' s disease ? *Nat. Cell Biol.* **2,** 115–119 (2000).
65. Giehm, L., Svergun, D. I., Otzen, D. E. & Vestergaard, B. Low-resolution structure of a vesicle disrupting alpha-synuclein oligomer that accumulates during fibrillation. *Proc. Natl. Acad. Sci. U. S. A.* **108,** 3246–51 (2011).
66. Reixach, N., Deechongkit, S., Jiang, X., Kelly, J. W. & Buxbaum, J. N. Tissue damage in the amyloidoses: Transthyretin monomers and nonnative oligomers are the major cytotoxic species in tissue culture. *Proc. Natl. Acad. Sci. U. S. A.* **101,** 2817–2822 (2004).
67. Hou, X. *et al.* Transthyretin oligomers induce calcium influx via voltage-gated calcium channels. *J. Neurochem.* **100,** 446–457 (2007).
68. Teixeira, P. F., Cerca, F., Santos, S. D. & Saraiva, M. J. Endoplasmic reticulum stress associated with extracellular aggregates: Evidence from transthyretin deposition in familial amyloid polyneuropathy. *J. Biol. Chem.* **281,** 21998–22003 (2006).
69. Monteiro, F. A. *et al.* Activation of ERK1/2 MAP kinases in familial amyloidotic polyneuropathy. *J. Neurochem.* **97,** 151–161 (2006).
70. Small, D. H., Mok, S. S. & Bornstein, J. C. Alzheimer's disease and Abeta toxicity:

from top to bottom. *Nat. Rev. Neurosci.* **2,** 595–8 (2001).

71. Holmgren L., *et al*. Biochemical effect of liver transplantation in two Swedish patients with familial amyloidotic polyneuropathy (FAP-met30). *Clin Genet.* **40,** 242–246 (1991).
72. Holmgren, G. *et al.* Clinical improvement and amyloid regression after liver transplantation in hereditary transthyretin amyloidosis. *Lancet.* **341,** 1113–1116 (1993).
73. Herlenius, G., Wilczek, H. E., Larsson, M.& Ericzon, B.-G. Ten years of international experience with liver transplantation for familial amyloidotic polyneuropathy: results from the Familial Amyloidotic Polyneuropathy World Transplant Registry. *Transplantation.* **77,** 64–71 (2004).
74. Stangou, A. J. *et al.* Progressive cardiac amyloidosis following liver transplantation for familial amyloid polyneuropathy: implications for amyloid fibrillogenesis. *Transplantation*. **66,** 229–233 (1998).
75. Olofsson, B. O., Backman, C., Karp, K. & Suhr, O. B. Progression of cardiomyopathy after liver transplantation in patients with familial amyloidotic polyneuropathy, Portuguese type. *Transplantation.* **73,** 745–751 (2002).
76. Liepnieks, J. J., Zhang, L. Q. & Benson, M. D. Progression of transthyretin amyloid neuropathy after liver transplantation. *Neurology.* **75,** 324–327 (2010).
77. Sebastião, M. P., Lamzin, V., Saraiva, M. J. M. & Damas, A. M. Transthyretin stability as a key factor in amyloidogenesis: X-ray analysis at atomic resolution. *J. Mol. Biol.* **306,** 733–744 (2001).
78. Johnson S., Connelly S., Fearns C., P. E. and K. J. The Transthyretin Amyloidoses: From Delineating the Molecular Mechanism of Aggregation Linked to Pathology to a Regulatory Agency Approved Drug. *J Mol Biol*. **421,** 185–203 (2012).
79. Miroy, G. J. *et al.* Inhibiting transthyretin amyloid fibril formation via protein stabilization. *Proc. Natl. Acad. Sci. U. S. A.* **93,** 15051–15056 (1996).
80. Harirforoosh, S., Asghar, W. & Jamali, F. Adverse effects of nonsteroidal antiinflammatory drugs: an update of gastrointestinal, cardiovascular and renal complications. *J Pharm Pharm Sci*. **16,** 821–47 (2013).
81. Sekijima, Y., Dendle, M. a & Kelly, J. W. Orally administered diflunisal stabilizes transthyretin against dissociation required for amyloidogenesis. *Amyloid.* **13,** 236–249 (2006).
82. Berk, J. L. *et al.* Repurposing Diflunisal for Familial Amyloid Polyneuropathy. *JAMA J. Am. Med. Assoc.* **310,** 2658–2667 (2013).
83. Nuernberg, B., Koehler, G. & Brune, K. Pharmacokinetics of Diflunisal in Patients. *Clin. Pharmacokinet.* **20,** 81–89 (1991).

84. Coelho L. F., *et al*. Tafamidis for transthyretin familial amyloid polyneuropathy: a randomized, controlled trial. *Neurology.* **79,** 785–792 (2012).
85. Merlini, G. *et al.* Effects of tafamidis on transthyretin stabilization and clinical outcomes in patients with non-Val30Met transthyretin amyloidosis. *J. Cardiovasc. Transl. Res.* **6,** 1011–1020 (2013).
86. Coelho, T. *et al.* Mechanism of Action and Clinical Application of Tafamidis in Hereditary Transthyretin Amyloidosis. *Neurol. Ther.* **5,** 1–25 (2016).
87. Li, Y. Y. & Jones, S. J. M. Drug repositioning for personalized medicine. *Genome Med*. **4,** (2012).
88. Leegwater-Kim, J. & Waters, C. Role of tolcapone in the treatment of Parkinson's disease. *Expert Rev Neurother*. **7,** 1649–1657 (2007).
89. Männistö, P. T. Clinical potential of Catechol-O-Methyltransferase (COMT) inhibitors as adjuvants in Parkinson's Disease. *CNS Drugs*. **1,** 172–179 (1994).
90. Reig, N., Ventura, S., Salvadó, M., Gámez, J. & Insa, R. SOM0226, a repositioned compound for the treatment of TTR amyloidosis. *Orphanet J. Rare Dis.* **10,** P9 (2015).
91. Freire, E., Schön, A. & Velazquez-Campoy, A. Chapter 5 Isothermal Titration Calorimetry. General Formalism Using Binding Polynomials. *Methods Enzymol.* **455,** 127–155 (2009).
92. Vega, S., Abian, O. & Velazquez-Campoy, A. A unified framework based on the binding polynomial for characterizing biological systems by isothermal titration calorimetry. *Methods*. **76,** 99–115 (2015).
93. Azevedo, E. P. C. *et al.* Dissecting the Structure, Thermodynamic Stability, and Aggregation Properties of the A25T Transthyretin (A25T-TTR) Variant Involved in Leptomeningeal Amyloidosis: Identifying Protein Partners That Co- Aggregate during A25T-TTR Fibrillogenesis in Cerebrosp. *Biochemistry*. **50,** 11070–11083 (2011).
94. Podoly, E., Hanin, G. & Soreq, H. Chemico-Biological Interactions Alanine-to-threonine substitutions and amyloid diseases : Butyrylcholinesterase as a case study. *Chem. Biol. Interact.* **187,** 64–71 (2010).
95. Levittl, M. Conformational Preferences of Amino Acids in Globular Proteins. *Biochemistry*. **17,** (1978).
96. Neurath, H. The role of glycine in Protein Structure. *J. Am. Chem. Soc.* **65,** 2039–2041 (1943).
97. Eneqvist, T. *et al.* Disulfide-Bond Formation in the Transthyretin Mutant Y114C Prevents Amyloid Fibril Formation in Vi V o and in Vitro. **55,** 13143–13151 (2002).
98. Hammarstro, P., Jiang, X., Deechongkit, S. & Kelly, J. W. Anion Shielding of

Electrostatic Repulsions in Transthyretin Modulates Stability and Amyloidosis : Insight into the Chaotrope Unfolding Dichotomy. *Biochemistry*. **40,** 11453–11459 (2001).

99. Jiang, X., Buxbaum, J. N. & Kelly, J. W. The V122I cardiomyopathy variant of transthyretin increases the velocity of rate-limiting tetramer dissociation , resulting in accelerated amyloidosis. *PNAS.* **98,** 14943–14948 (2001).
100. Anna, R. S. *et al.* Cavity filling mutations at the thyroxine-binding site dramatically increase transthyretin stability and prevent its aggregation. *Sci. Rep.* **7,** 1–15 (2017).
101. Pullakhandam, R., Srinivas, P. N. B. S., Nair, M. K. & Reddy, G. B. Binding and stabilization of transthyretin by curcumin. *Arch. Biochem. Biophys.* **485,** 115–119 (2009).
102. Foss, T. R., Kelker, M. S., Wiseman, R. L., Wilson, I. A. & Kelly, J. W. Kinetic Stabilization of the Native State by Protein Engineering : Implications for Inhibition of Transthyretin Amyloidogenesis. *J. Mol. Biol.* **347,** 841–854 (2005).
103. Perozzo, R., Folkers, G. & Scapozza, L. Thermodynamics of Protein – Ligand Interactions : History , Presence , and Future Aspects. *J. Recept. Signal Transduct.* **24,** 1–52 (2004).
104. Du, X. *et al.* Insights into Protein-Ligand Interactions: Mechanisms, Models, and Methods. *Int. J. Mol. Sci.* **17,** 144 (2016).
105. Pierce, M. M., Raman, C. S. & Nall, B. T. Isothermal Titration Calorimetry of Protein – Protein Interactions. *Methods* **19,** 213–221 (1999).
106. Mccammon, M. G. *et al.* Screening Transthyretin Amyloid Fibril Inhibitors : Characterization of Novel Multiprotein , Multiligand Complexes by Mass Spectrometry. *Structure.* **10,** 851–863 (2002).
107. Wiseman, R. L. *et al.* Kinetic Stabilization of an Oligomeric Protein by a Single Ligand Binding Event. *J. Am. Chem. Soc.* **127,** 5540–5551 (2005).
108. Kolstoe, S. E. *et al.* Trapping of palindromic ligands within native transthyretin prevents amyloid formation. *PNAS* **107,** 20483–20488 (2010).
109. Green, N. S., Palaninathan, S. K., Sacchettini, J. C. & Kelly, J. W. Synthesis and Characterization of Potent Bivalent Amyloidosis Inhibitors That Bind Prior to Transthyretin Tetramerization. *J. Am. Chem. Soc.* **124,** 13404–13414 (2003).
110. Reynolds, C. H. & Holloway, M. K. Thermodynamics of Ligand Binding and Efficiency. *ACS Med. Chem. Lett.* **2,** 433–437 (2011).
111. Chodera, J. D. & Mobley, D. L. Entropy-enthalpy compensation: Role and ramification in biomolecular ligand recognition and design. *Annu Rev Biophys* **42,** 121–142 (2013).
112. Lafont, V. *et al.* Compensating Enthalpic and Entropic Changes Hinder Binding

Affinity Optimization. *Chem Biol Drug Des* **69,** 413–422 (2007).

113. Gales, L., Macedo-ribeiro, S., Arsequell, G., Valencia, G. & Jo, M. Human transthyretin in complex with iododiflunisal : structural features associated with a potent amyloid inhibitor. *Biochem J.* **388,** 615–621 (2005).
114. Adamski-werner, S. L., Palaninathan, S. K., Sacchettini, J. C. & Kelly, J. W. Diflunisal Analogues Stabilize the Native State of Transthyretin . Potent Inhibition of Amyloidogenesis. *J. Med. Chem.* **47,** 355–374 (2004).
115. Schneider, F., Öm, P. E. R. H. & Kelly, J. W. Transthyretin slowly exchanges subunits under physiological conditions : A convenient chromatographic method to study subunit exchange in oligomeric proteins. *Protein Sci.* **10,** 1606–1613 (2001).
116. Verona, G. *et al.* Inhibition of the mechano- enzymatic amyloidogenesis of transthyretin : role of ligand affinity , binding cooperativity and occupancy of the inner channel. *Sci. Rep.* **7,** 1–7 (2017).